Instytut Fizyki Molekularnej
Polskiej Akademii Nauk

MONOGRAFIA

Iwona Olejniczak

Charge localization and superconductivity in optical investigations of low-dimensional organic conductors including different functionalities

Poznań
2021

Iwona Olejniczak
Charge localization and superconductivity in optical investigations of low-dimensional organic conductors including different functionalities

Wydawca:
Instytut Fizyki Molekularnej Polskiej Akademii Nauk©
Mariana Smoluchowskiego 17
60-179 Poznań
Rok wydania: 2021

ISBN: 978-83-956445-6-6

Charge localization and superconductivity in optical investigations of low-dimensional organic conductors including different functionalities

Iwona Olejniczak

Institute of Molecular Physics Polish Academy of Sciences,
Smoluchowskiego 17, 60-179 Poznań, Poland

ABSTRACT

Low-dimensional organic solids have emerged in the last century as a result of the rapid development of chemical technology and a quest for high-temperature superconductivity. It became apparent quite early that their physical properties were characterized by strong anisotropy and the ground state depended on the complex electron-electron and electron-fonon interactions as well as the details of the molecular structure. This review is focused on optical properties of organic conductors. In particular, some properties related with localization of charge are revealed in selected experiments on low-dimensional organic materials.

Contents

1. Introduction

Since their early days, people have been searching for useful materials with characteristics desired at a given stage of civilization development. Subsequent discoveries were made at irregular intervals, until the last century, when the rapid development of chemical technology made it possible to synthesize solids with previously unknown, unique properties. Many new organic materials appeared then, such as polymers, fullerenes, carbon nanotubes and graphene, as well as organic low-dimensional semiconductors and conductors. It became apparent quite early that their physical properties were characterized by strong anisotropy and the ground state depended on the complex electron-electron and electron-fonon interactions as well as the details of the molecular structure. They exhibit a number of properties that are important from the point of view of applications, such as high electrical conductivity, metal-insulator phase transition, magnetic order and superconductivity, which can be modified by small modifications of external parameters: temperature, pressure, magnetic or electric field. Low-dimensional organic materials have rather poor mechanical properties but the inexpensive synthesis and simplicity of obtaining new materials by chemical modifications of the existing ones is their undoubted advantage. Therefore, the possibilities of applications in modern industry are still being sought for them [1]. On the other hand, due to the unique opportunity for testing theoretical models describing various ground states under conditions of reduced dimensionality, these materials raise unwavering interest of researchers.

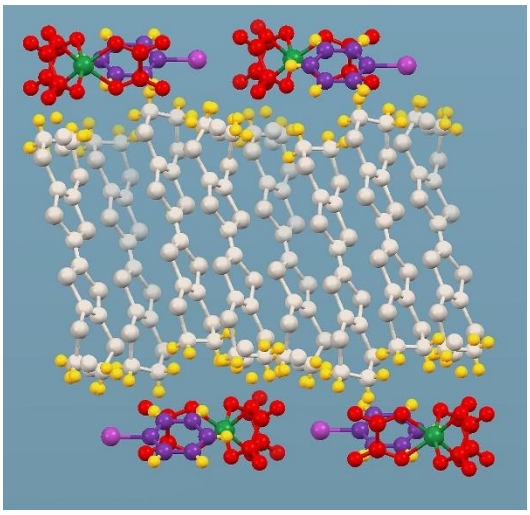

Figure 1: Layered BEDT-TTF structure shown on the example of the β′′-(BEDT-TTF)$_4$[(H$_3$O) Fe(C$_2$O$_4$)$_3$]·Y salt. BEDT-TTF molecules are marked with the light color (Adapted with permission from [101]. Copyright 2013 Wiley-VCH Verlag GmbH & Co. KGaA, Weinheim).

A historically important stimulus for the development of this field of low-dimensional organic conductors was the work of W. Little, who suggested the possibility of obtaining high-temperature superconductivity in this group of materials [2]. The intensive search initiated in this way led to the discovery of the first organic superconductors (TMTSF)$_2$PF$_6$ at the increased pressure [3] (TMTSF = tetramethylotetraselenafulvalene), and (TMTSF)$_2$ClO$_4$ with the temperature of transition to the superconducting phase at normal pressure T_c = 1.4 K [4]. The present work is concerned with another family of organic conductors characterized by superconducting properties, the two-dimensional (2D) materials based on the flat BEDT-TTF (bis (ethylenedithio)tetrathiafulvalene) donor molecule or its derivatives [5]. In these salts, conducting donor layers are arranged alternately with non-conducting anion layers (Fig. 1), and delocalization of charge carriers within the conducting layers is due to the

overlap of partially filled π molecular orbitals of the donor molecules. Increased electrical conductivity occurs in the direction of the largest overlap, and the filling of the conducting band depends on the charge transferred between the donor and acceptor molecules. In particular, the salts with the general formula (BEDT-TTF)$_2$X, where X is a charge compensating ion, and the formal ¼ band filling in the hole conductivity description, have been of interest since many years. The ground state in these model conducting systems depends on the subtle balance of several factors, including the most important Coulomb interactions U between charge carriers localized on the same donor molecule or V between adjacent donor molecules [5-7], that are strong in comparison with the width of the conducting band. In strongly dimerized systems with effective ½ band filling, the interactions of unpaired spins lead to the stabilization of the insulating dimer Mott (DM) state (Fig. 2) or superconductivity (SC) [8]. Here, a model example is the κ-(BEDT-TTF)$_2$Cu[N(CN)$_2$]Br superconductor with the temperature of transition to the superconducting phase T_c = 11.6 K, the highest in this group of materials [9,10].

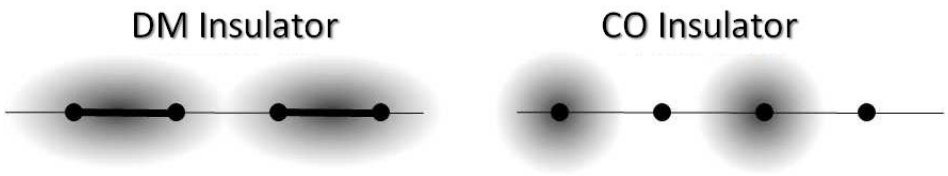

Figure 2: Schematic view of the insulating dimer Mott (DM, left) and charge ordered (CO, right) states. The molecules are illustrated with the black dots, the dimers - with the thickened line segments between molecules. The localized electric charge is shown with grey color.

On the other hand, in weakly dimerized (BEDT-TTF)$_2$X salts the insulating ground state with charge order (CO) is observed (Fig. 2) [11-13]. The CO state is related with the presence of significant Coulomb V interactions and is intensively studied because of the possible connection with the appearance of superconductivity in this group of materials [14]. Recently it has been shown, both theoretically and experimentally, that in some (BEDT-TTF)$_2$X salts the charge ordered state, which is sometimes dynamic in case of so-called charge fluctuations, coexists with the insulating Mott state [15-19]. Such electric dipoles within dimers can result in the appearance of electronic ferroelectricity (FE) [20-22]. They are also related with the low temperature stabilization of the Quantum Dipole Liquid (QDL), recently demonstrated in case of the Mott insulator κ-(BEDT-TTF)$_2$Hg(SCN)$_2$ [23]. This exotic state of matter associated with the presence of electric dipoles fluctuating to the lowest measurable temperatures may coexist, in the presence of charge and spin coupling, with Quantum Spin Liquid (QSL), which was observed in case of two other materials of this group, κ-(BEDT-TTF)$_2$Ag$_2$(CN)$_3$ and κ-(BEDT-TTF)$_2$Cu$_2$(CN)$_3$ [24,25].

Although the knowledge of ground states in low-dimensional organic conductors has recently expanded not all issues have been clarified. One of the questions is the role of structural disorder, which can be present in the (BEDT-TTF)$_2$X salts both in the anion and the conducting donor layers [26,27]. An important direction of research is also the search for new materials with useful properties, composed of different molecules than those used so far. For example, molecules containing magnetic ions [28-30] or chiral molecules [31] are used in synthesis to obtain multifunctional materials. Nevertheless, further development of organic conductors requires a thorough understanding of the role of all interactions

affecting the physical properties of the material and involved in phase transitions. Current directions in the field of organic conductors with two-dimensional structure are shown in the diagram below (Fig. 3).

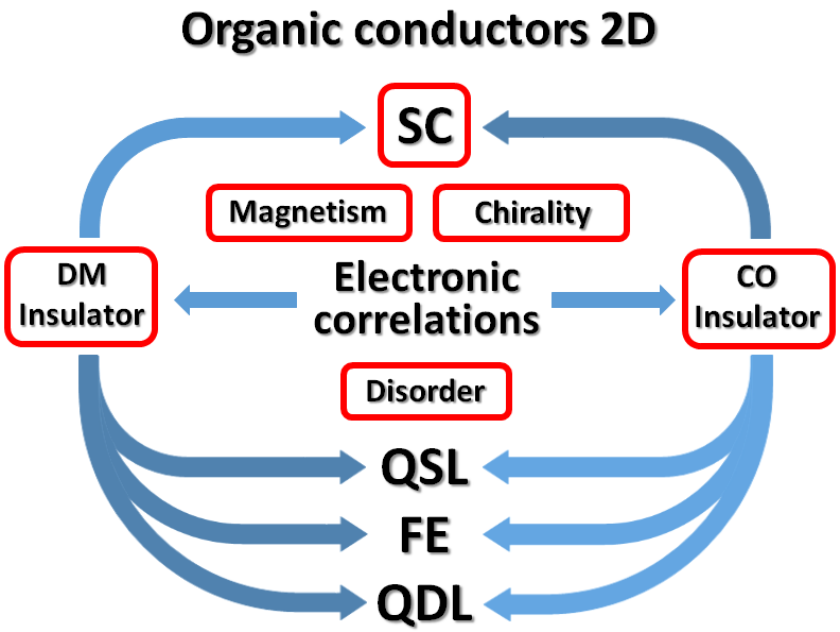

Figure 3: Research directions in the field of 2D organic conductors: dimer Mott (DM) insulator, charge ordered (CO) insulator, superconductivity (SC), quantum spin liquid (QSL), electron ferroelectricity (FE), quantum dipole liquid (QDL), magnetism, chirality, (structural) disorder. Red frames denote issues that are relevant to the research presented in this work.

This review of selected studies performed using optical spectroscopy methods is a contribution to this area of research. Optical spectroscopy is a microscopic research tool providing precise information on the electronic structure as well as on the local electron-electron and electron-phonon interactions in a material. In particular, the middle-infrared spectra allow determination of the energy gaps and transfer integrals, which are responsible for electrical conductivity of the system. At the same time, the charge distribution on molecules can be determined from vibrational spectra.

2. Optical properties of organic conductors

The physical properties of low-dimensional organic conductors can be described in a convenient way using the Hamiltonian proposed by J. Hubbard in 1963 [32], which is a simplified model used for systems characterized by a single, narrow conductivity band near the Fermi surface. This model correctly describes metallic states, metal-insulator phase transitions and magnetic properties of low-dimensional systems. In its simplest form, the Hubbard model considers only the hopping (transfer) integral t, which is a measure of kinetic energy of the charge carriers, and the Coulomb U interaction between charge carriers on the same lattice site.

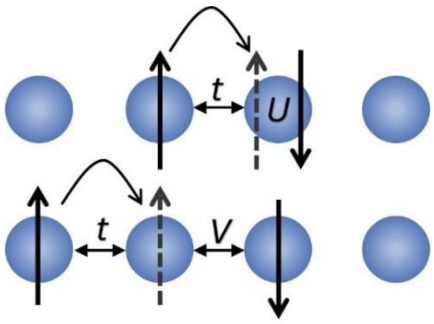

Figure 4: Schematic representation of a one-dimensional chain of lattice sites with quarter filling, with the most important interactions labeled as follows: t - the transfer integral, U (top row) - Coulomb interactions on the same site, V (bottom row) - Coulomb interactions between adjacent sites.

More useful formula takes into account a term related to Coulomb repulsion V between electrons on the neighboring lattice sites as it is very important from the point of view of stabilization of the charge ordered state [33-35]:

$$H = \sum_{\langle ij\rangle,\sigma} t_{\langle ij\rangle}(c^{\dagger}_{i,\sigma}c_{j,\sigma} + c^{\dagger}_{j,\sigma}c_{i,\sigma}) + U\sum_{i} n_{i,\uparrow}n_{i,\downarrow} + \sum_{\langle ij\rangle} V_{ij}n_i n_j \qquad (1)$$

where *i* and *j* define network sites, <*ij*> means a pair of network sites, σ is a spin parameter assuming the values ↑ and ↓, $t_{<ij>}$ is the hopping integral defined for a pair of lattice sites, $n_{i,\uparrow}$ and $n_{i,\downarrow}$ are particle number operators, $c^{\dagger}_{i,\sigma}$ and $c_{i,\sigma}$ are creation and annihilation operators, respectively. The hopping integral *t* is a function of intermolecular distances of r_{ij} and mutual orientation of molecular orbitals. In case of organic conductors, *t* is a value of the order of 100 meV [36] decreasing exponentially with the increase of r_{ij}, and the Coulomb interactions U and V are about an order of magnitude larger [5], while V ~ 1/ r_{ij}. The physical sense of Hubbard model parameters in relation to a one-dimensional chain of evenly distributed molecules with the quarter filling of the conducting band is shown in Figure 4.

Let us consider the case of the Hubbard model for V = 0. Such a system is a metal in the limiting case U = 0. In the second limiting case U >> t, the electric charge is located evenly on the lattice sites. Such a ground state is called the Mott insulator and depends on the band filling; it appears in systems with ½ band filling characteristic for dimerized systems (Fig. 2). If the Coulomb repulsion V is significant that takes place in weakly dimerized systems with ¼ band filling, electrons become localized in the insulator state on every second lattice site in the charge ordered state (Fig. 2).

a. Electronic excitations

In classical metals the metallic state is described by the Drude model, in which it is assumed that electrons do not interact with each other and move freely according to Newton's laws until they scatter from the lattice and impurities. Considering no Coulomb interactions in the system (U = 0), there is only one band at Fermi level related to free charge carriers described by the Drude function, with Density of States (DOS) concentrated around the maximum of this band. The optical conductivity spectrum of such a metal consists of one Drude peak at frequency ω = 0 (Fig. 5, left). In the Hubbard model,

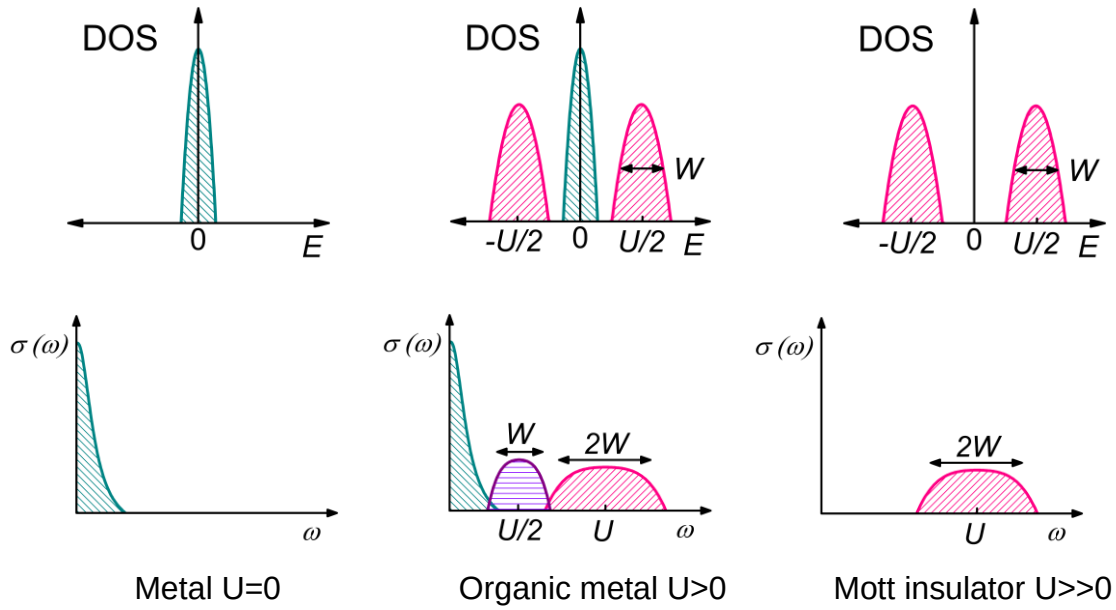

Figure 5: Density of states (DOS) and corresponding spectra of optical conductivity for metal (left), organic conductor (center) and Mott's insulator (right) described by the Hubbard model. U denotes Coulomb interaction on the same lattice site, while W - bandwidth (after Rozenberg et al. [37]).

the density of states for organic metal consists of a similar band at the Fermi level and two Hubbard bands separated by an energy gap of the width U. In such a system, in the optical conductivity spectrum in addition to the Drude peak there is a wide band at frequency U called the Hubbard band, associated with the transition between the two Hubbard bands in DOS. It is also possible that an additional band appears for the frequency U/2 related to the transitions between the Hubbard bands and the middle band of free charge carriers (Fig. 5, center) [37]. In the case of Mott insulator, there are only two Hubbard bands in the density of states for the Hubbard model, so the transitions between them generate one absorption band for the frequency U in the optical conductivity spectrum (Fig. 5, right) [37].

In real materials with 1/4 band filling, which are more or less dimerized, HOMOs (High Occupied Molecular Orbitals) of single molecules form dimer orbitals, which are subject to splitting into bonding and anti-bonding orbitals. This leads to the appearance of the dimer band, an additional absorption band in the middle infrared, which is due to the electronic transition within the dimer between the energy levels of the bonding and anti-bonding orbitals (Fig. 6) [38-40]. Electron correlations do not influence the dimer band; it usually appears in the spectrum at a slightly higher frequency than the Hubbard band related with correlations, which frequency allows estimation of the effective Coulomb U interaction on the dimer. The shape of the spectrum strongly depends on the degree of dimerization. In weakly dimerized systems both the Hubbard and the dimer bands form a single band shifted towards lower frequencies below 2500 cm^{-1}. On the other hand, in the case of strong dimerization the dimer band is shifted significantly above the Hubbard band, with the maximum located at the frequency corresponding to doubled value of the transfer integral t_D in the dimer [18].

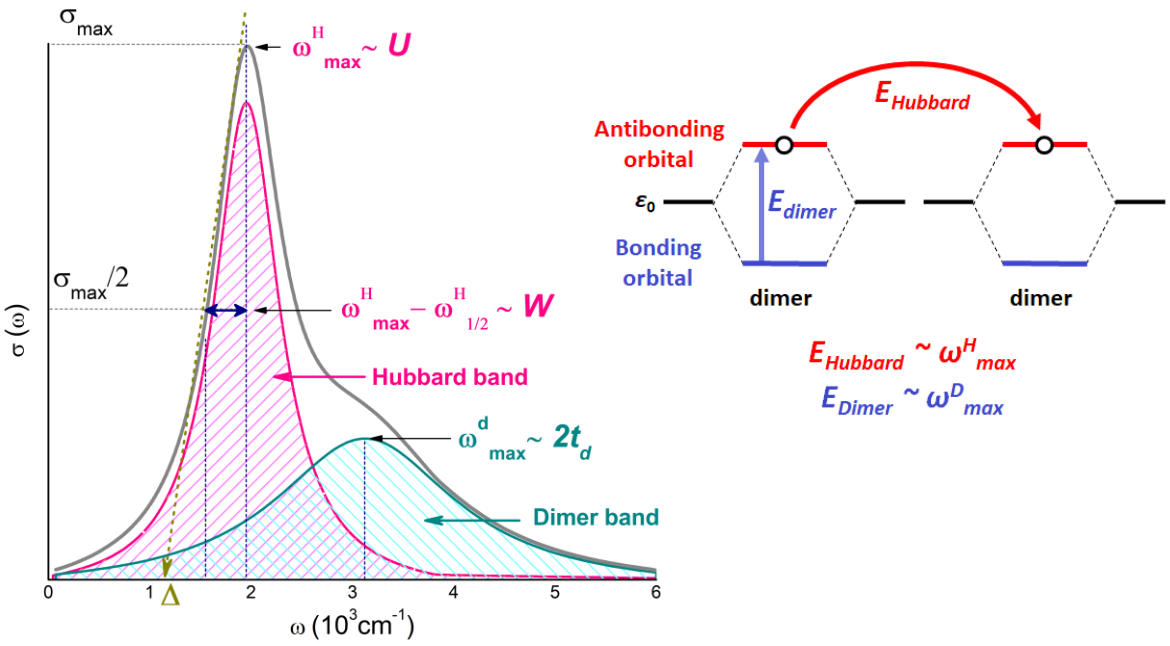

Figure 6: The optical conductivity spectrum of dimer Mott insulator (left). Two components of the electronic band observed in medium infrared are shown: the Hubbard band associated with charge transfer between dimers and the Dimer band associated with charge transfer within the dimer. In the figure, the most important parameters are identified: energy gap Δ, frequency in the maximum of the Hubbard band ω_{Hmax}, which value is determined by the value of Coulomb U interactions, its half width ω_{Hmax}-$\omega_{H1/2}$, which corresponds to the bandwidth W, and also the frequency in the maximum of the dimer band ω_{Dmax}, which in strongly dimerized systems corresponds to the value $2t_D$, where t_D is the transfer integral within the dimer. A simplified diagram of electronic transitions between the dimer bonding and anti-bonding orbitals related to the Dimer band (E_{Dimer}), and Hubbard band ($E_{Hubbard}$) is shown on the right.

The charge order insulating state occurs in correlated materials with significant Coulomb V interactions. It does not depend on the dimensionality of the system, and, unlike Mott insulator, it is not associated with any characteristic electronic response in the middle infrared. The shape of the electronic band in this case depends on the arrangement in the structure of charge-rich and charge-poor molecules, which can form stripes (vertical, horizontal or diagonal) or checkerboard [41,42]. Characteristic electronic bands related to CO or CO fluctuations may appear in the far infrared spectra [43,44], but such studies go beyond the subject matter of this paper. Very characteristic for the CO state are specific vibrational bands with frequency depending on the charge localized on the oscillating molecule. They are discussed in detail in the next subsection.

b. Charge-sensitive vibrational modes

In infrared spectra of $(BEDT\text{-}TTF)_2X$ salts, in addition to electronic bands associated with charge transfer, relatively strong bands are observed, mostly related to intramolecular vibrational modes of the BEDT-TTF donor molecule. Some of the modes are normally infrared active due to their symmetry. Other features, related to totally symmetrical vibrations that in the case of isolated molecules can be observed only in the Raman spectra, in organic conductors appear in the infrared spectra due to the coupling with charge transfer, the so-called electron-intramolecular vibration (EMV) coupling, as strong broadened bands shifted towards lower frequencies in comparison with the frequency of a corresponding mode in the Raman spectrum. EMV coupling is due to the fact that some vibrations dynamically

modulate the energy of molecular HOMOs and may therefore affect the charge transfer between molecules in the conducting layer. Such a coupling within the dimer results in the formation of an oscillating dipole [45], the phenomenon explained on the basis of the dimer model [46]. It is the centrosymmetric out-of-phase vibrations of the dimer components that are subject to EMV coupling according to the model. For each fully symmetrical mode the coupling effect depends on its electron-intramolecular vibrations coupling constant. In case of BEDT-TTF donor molecule particularly strong coupling is observed for a stretching mode labeled as ν_3 in D_{2h} symmetry, mainly involving the central double C=C bond (Fig. 7). The downshift of the ν_3 band in the infrared spectrum in relation to its frequency in the Raman spectrum strongly depends on the transfer integrals in the nearest vicinity of the oscillating molecule [47]. Therefore, the frequency of ν_3 depends on local structure and can be used to study phase transitions in the material.

ν_3 mode and two other stretching vibrations of the double C=C bonds are also sensitive to the charge localized on the BEDT-TTF molecule. This is a result of the dependence of the C=C bond length on the charge [48]. The bond lengths can be determined based on structural studies, but the value of the charge estimated by this method is subject to an error of the order of 0.1e, or even larger than that in case of materials with structural disorder [49]. Moreover, X-ray examinations give results averaged over the whole sample. In fact, a much more accurate method that allows estimation of charge localized on the molecule is the observation of bands of appropriate molecular vibrations in the infrared (IR) and Raman vibrational spectra. Due to the frequency range of vibrational spectroscopies, this method is microscopic and can be used to study not only the long-range charge arrangement, but also local fluctuations accompanying phase transitions [50]. If all donor molecules in a BEDT-TTF-based salt are equivalent, the charge on each donor molecule is the same and a single intramolecular mode results in one band observed in vibrational spectrum. A different situation occurs in the charge ordered state when the charge on molecules is distributed unevenly. In such a case there are molecules rich in charge (R) and molecules poor in charge (P) in the structure, and a selected vibrational mode is split into two components. If the charge in the system fluctuates around certain value, then instead of splitting, the bands broadened according to the rate and amplitude of the fluctuation are observed. Two components of such a band can be separated using the "two-states-jump-model" model proposed by Kubo [51].

Considering flat D_{2h} symmetry for BEDT-TTTF molecule characterized by three double C=C bonds, there are three stretching vibrations involving these bonds, two totally symmetric modes ν_2 (A_g) and ν_3 (A_g) observed in Raman's spectra, and unsymmetrical (ungerade) infrared active ν_{27} (B_{1u}) mode (Fig. 7), that display splitting in the CO state. It was shown that frequencies of these three modes decrease significantly between the neutral and charged molecules [52,53], but the two A_g modes are also involved in EMV coupling making the picture more complicated. The ν_2 mode observed in Raman spectra is only slightly disturbed by EMV coupling; the dependence of its frequency on charge is linear for a wide range of charges, therefore the ν_2 band can be used to study CO states. On the other hand, the ν_3 mode is so much coupled with the electrons that its splitting in the CO state is determined by the EMV coupling rather than by the fractional charge. ν_3 may also influence the ν_2 mode components in the crystal network conditions [54]. The theoretical calculations of the ν_2 and ν_3 frequencies for a particular structural unit, such as tetramer [54] or stacks of differently charged molecules (Fig. 7) [50], show that the frequency ν_{3P} for a charge-poor molecule is disturbed and corresponds to an average charge of 0.5e [54]. The frequency of the ν_{2R} band usually differs from the linear dependence for $\Delta\rho > 0.2$, but this effect depends on the magnitude of the interactions characteristic for a given structure. For larger $\Delta\rho$,

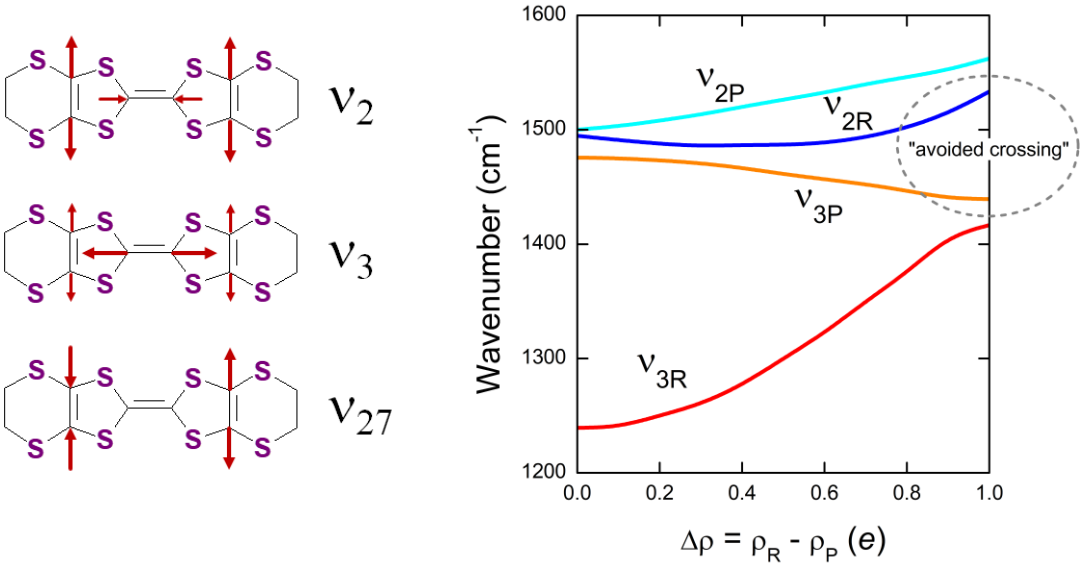

Figure 7: On the left: stretching vibrations of BEDT-TTF molecules in D_{2h} symmetry observed in Raman (ν_2 and ν_3) and in infrared spectra (ν_{27}). Stretching of the central double C=C bond gives a small contribution to the ν_2 mode, and stretching of the lateral C=C bonds a small contribution to the ν_3 mode. On the right: the frequencies of ν_2 and ν_3 components of charge-rich (ν_{2R}, ν_{3R}) and charge-poor (ν_{2P}, ν_{3P}) molecules as a function of charge difference $\Delta\rho = \rho_R - \rho_P$ (ρ_R denotes charge of the molecule rich in charge, ρ_P - charge of the molecule poor in charge) calculated for the β′′-type structure with differently charged stacks of BEDT-TTF molecules (after Girlando et al. [50]).

the so-called "avoided crossing" effects cause distortion of both ν_{2R} and ν_{3P} dependencies on charge (Fig. 7). The ν_{2P} frequency for a molecule poor in charge is undisturbed (Fig. 7), but its band in the Raman spectrum is rather weak. In order to calculate the charge based on the ν_2 mode components, we use a linear relationship (in cm^{-1}) [54]:

$$\nu_2(\rho) = 1447 + 120(1 - \rho) \tag{2}$$

The best spectroscopic probe of charge localized on the molecule is the ν_{27} mode, which is normally infrared active and not involved in EMV coupling. The dipole moment associated with this vibration is parallel to the long axis of the BEDT-TTF molecule [55,56], therefore the ν_{27} band can be observed in most materials in the direction perpendicular to the best developed plane of the single crystal. Such experiment involves a difficulty of probing a narrow side wall of the sample. In order to calculate the charge based on the ν_{27} band components, we use the linear relation (in cm^{-1}) [54]:

$$\nu_{27}(\rho) = 1398 + 140(1 - \rho) \tag{3}$$

3. Materials and research methodology

This review is focused on three families of organic conductors. All these materials are characterized by the presence of conducting two-dimensional donor layers.

a. κ-(BEDT-TTF)$_2$X salts

Several well-known organic superconductors crystallizing in the κ-phase (table below) were selected for measurements of vibrational spectra in strong magnetic fields (see table below). These salts are characterized by the highest temperatures of superconducting phase transition in this group of materials.

Formula	Critical temperature	Reference
κ-(BEDT-TTF)$_2$Cu(SCN)$_2$,	T_c = 10.4 K	[57]
κ-(BEDT-TTF)$_2$Cu[N(CN)$_2$]Br,	T_c = 11.6 K	[9]
κ-(BEDT-TTF)$_2$Cu[N(CN)$_2$]Cl,	T_c = 12.8 K under pressure 0.3 kbar	[58]

In the conducting layer of the κ type there are no clearly distinguished stacks of BEDT-TTF molecules, as it is formed by orthogonally arranged, interacting dimers (Fig. 8).

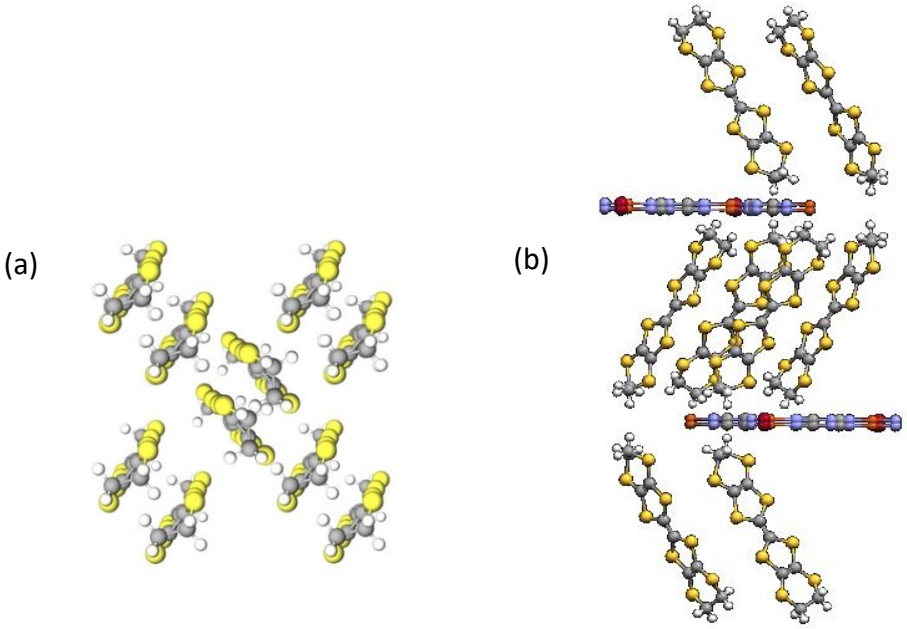

Figure 8: Conducting κ-type layer (a), and layered structure of the κ-(BEDT-TTF)$_2$Cu[N(CN)$_2$]Br salt (b).

Two of the materials were κ-$(BEDT\text{-}TTF)_2Cu(SCN)_2$ salts with isotopic substitutions in the BEDT-TTF donor molecule. Deuterium, carbon ^{13}C and sulfur ^{34}S atoms were used for substitutions, as shown below in Fig. 9.

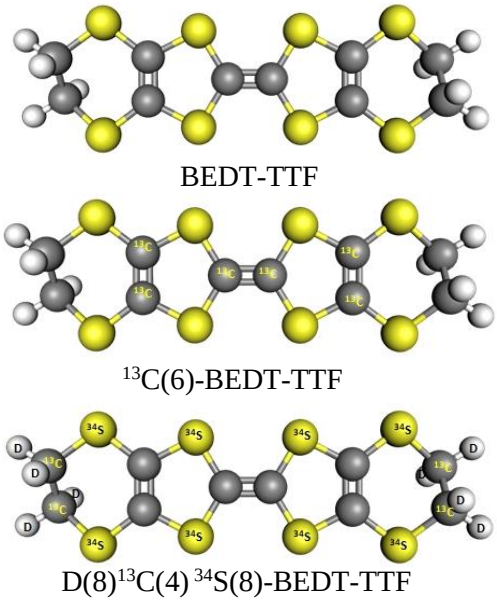

Figure 9: Molecular structure of BEDT-TTF (top) and two other variants with isotopic substitutions: $^{13}C(6)$-BEDT-TTF (middle) and $D(8)^{13}C(4)^{34}S(8)$-BEDT-TTF (bottom).

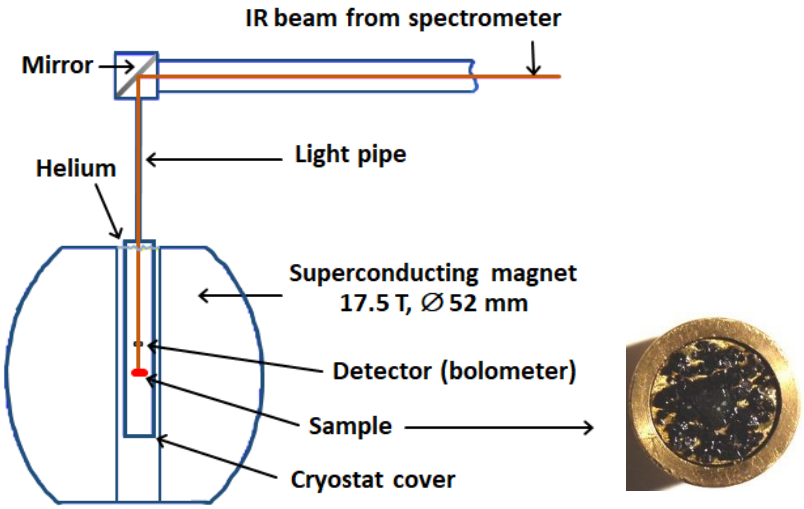

Figure 10: A diagram of the magnetic field experiment together with a photograph of the sample mounted for reflectance spectra acquisition that is a mosaic of monocrystals glued to a metal substrate with a diameter of 9.5 mm.

The measurements were performed at the National High Magnetic Field Laboratory in Tallahassee, USA, using infrared reflectance spectroscopy in magnetic field. Figure 10 shows a simplified diagram of the experimental setup with a probe placed in the magnetic field, and a mosaic sample with a diameter of 9.5 mm. The measurements were performed at the temperature 4.2 K, in the frequency range 30-2500 cm^{-1} and magnetic fields 0-17 T. The magnetic field was perpendicular to the conducting plane of the sample.

b. β′′- and β′-phase BEDT-TTF salts

In BEDT-TTF salts crystallizing in the β′′-phase, the conducting layers are composed of stacks of regularly arranged donor molecules with planes inclined in respect to the column axis. Due to the presence of short sulphur-sulphur contacts between the columns, the interactions have a two-dimensional character. The majority of materials of this group have conducting band filled in ¼ and exhibit metallic conductivity at room temperature [59]. Due to the small dimerization, the insulator state is usually related with charge ordering [60]. On the other hand, the β′-type packing is characterized by dimerized stacking of BEDT-TTF molecules and mostly one-dimensional interactions within the conducting plane.

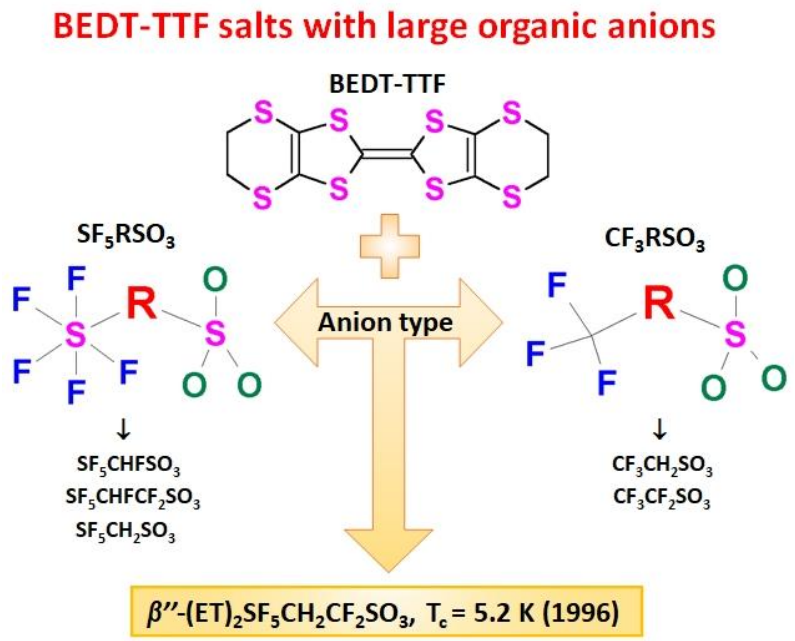

Figure 11: The large organic anion variants used in synthesis of salts with the general formula (BEDT-TTF)$_2$R1R2SO$_3$.

β′′-(BEDT-TTF)$_2$SF$_5$CHFCF$_2$SO$_3$, β′′-(BEDT-TTF)$_2$SF$_5$CHFSO$_3$, β′′-(BEDT-TTF)$_2$SF$_5$CH$_2$SO$_3$, β′′-(BEDT-TTF)$_2$CF$_3$CH$_2$SO$_3$ and β′-(BEDT-TTF)$_2$CF$_3$CF$_2$SO$_3$ belong to the family of BEDT-TTF-based materials with organic anions that incorporate a sulfonic R-SO$_3$ group (Fig. 11). These discrete anions are easy to modify chemically. They also form numerous hydrogen bonds with the ending ethylene groups of the BEDT-TTF donor molecule in the conducting layer, which can be important for the stabilization of a specific ground state in the material [61,62]. Numerous salts of this group were synthesized as a result of the search for superconductivity, after discovering in 1996 the β′′-(BEDT-TTF)$_2$SF$_5$CH$_2$CF$_2$SO$_3$ conductor that develops a superconducting state at 5.2 K [63]. In later studies it was suggested that superconductivity in this material is related to the presence of charge order fluctuations [12,14,45]. The β′′-(BEDT-TTF)$_2$SF$_5$CHFCF$_2$SO$_3$ and β′′-(BEDT-TTF)$_2$SF$_5$CHFSO$_3$ salts that exhibit metallic properties at room temperature, share a similar structure with the β′′-(BEDT-TTF)$_2$SF$_5$CH$_2$CF$_2$SO$_3$ superconductor. In contrast, two isostructural salts β′′-(BEDT-TTF)$_2$SF$_5$CH$_2$SO$_3$ and β′′-(BEDT-TTF)$_2$CF$_3$CH$_2$SO, together with the β′-(BEDT-TTF)$_2$CF$_3$CF$_2$SO$_3$ dimer Mott insulator displays low electrical conductivity in the whole temperature range (Fig. 12) [61,64].

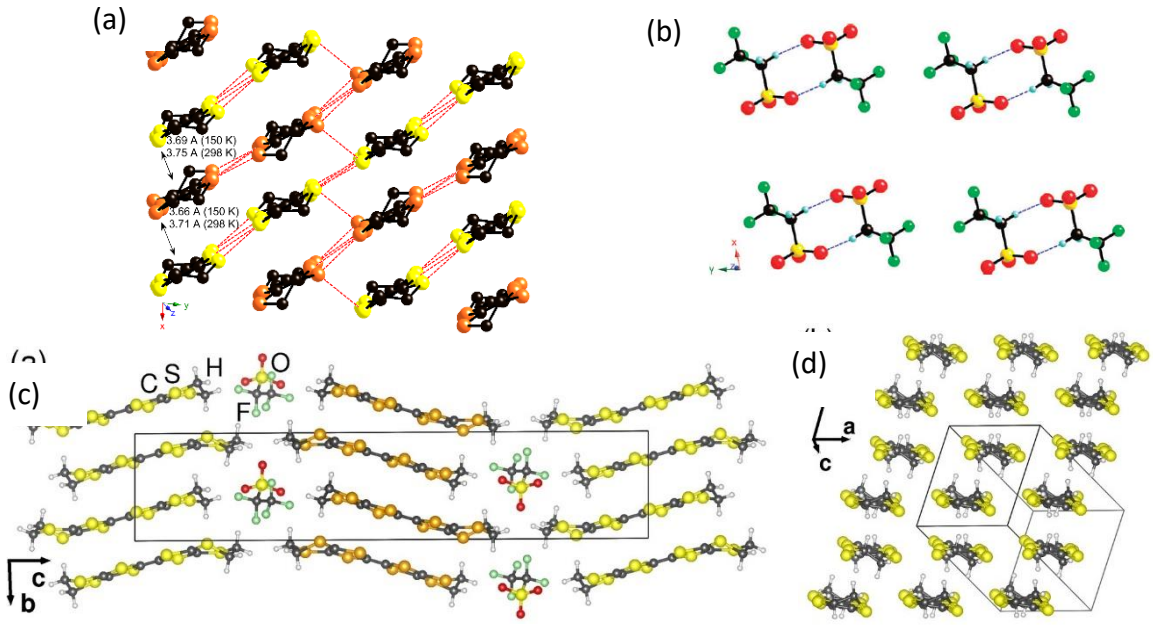

Figure 12: Structural details of selected BEDT-TTF salts with tunable organic anion. (a) Conducting layer, and (b) packing pattern of the anion layer of β′′-(BEDT-TTF)$_2$CF$_3$CH$_2$SO$_3$ (Reprinted with permission from [65]. Copyright 2009 Royal Society of Chemistry); (c) packing diagram and (d) conducting layer of β′-(BEDT-TTF)$_2$CF$_3$CF$_2$SO$_3$ (Reprinted with permission from [64]. Copyright 2020 American Physical Society). Note that sulfur atoms in two independent BEDT-TTF molecules, A and B, are marked in yellow and orange colors, respectively in (b) and (c) panels.

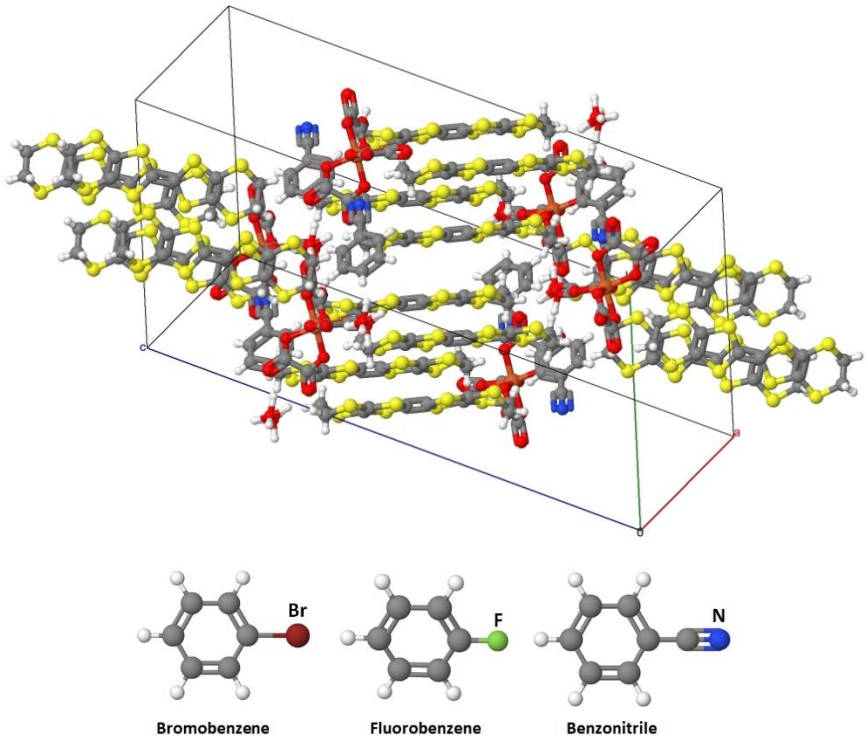

Figure 13: Packing diagram of β′′-(BEDT-TTF)$_4$[(H$_3$O)Fe(C$_2$O$_4$)$_3$]·Y (CCDC Ref. 771733), where Y denotes a solvent molecule: bromobenzene, fluorobenzene or benzonitrile (shown in the bottom).

The β′′-(BEDT-TTF)$_4$[(H$_3$O)Fe(C$_2$O$_4$)$_3$]·Y salts, where Y = C$_6$H$_5$Br, (C$_6$H$_5$CN)$_{0.17}$ (C$_6$H$_5$Br)$_{0.83}$, (C$_6$H$_5$CN)$_{0.4}$(C$_6$H$_5$F)$_{0.6}$, were synthesized in the search for bifunctional materials combining magnetic

properties with superconductivity [28-30]. The characteristic feature of these materials is the anion layer based on complex tris(oxalato)ferrate anions forming a hexagonal honeycomb structure with neutral molecules of solvent placed in the open spaces (Fig. 13). These materials exhibit metallic properties and superconductivity at low temperature [66-70], and the size and character of the solvent molecule [67,71-73] have a major influence on the stabilization of a particular ground state. All investigated materials are superconductors at low temperature (T_c = 4 - 6 K) and show structural phase transition in the temperature range 160 - 230 K [69,70,74]. A packing diagram of the β′′-(BEDT-TTF)$_4$[$(H_3O)Fe(C_2O_4)_3$]·Y material is shown in Figure 13, together with solvent molecules used in synthesis.

c. Salts of chiral tetrathiafulvalene derivatives

Another route to develop new low-dimensional organic conductors is the introduction of chirality through the use of chiral tetrathiafulvalene derivatives as donor in the synthesis [31]. Figure 14 shows chiral EDO-(*S*,*S*)-DMEDT-TTF (ethylenedioxy-(*S*,S)-dimethylethylene-dithio-tetrathiafulvalene) molecule that has been used in synthesis and molecular structure of the chiral τ-(EDO-(*S*,*S*)-DMEDT-TTF)$_2$($AuBr_2$)($AuBr_2$)$_y$ salt. Asymmetrical donor molecules are usually arranged in the "head-tail" manner in the structure, and such a procedure allows to obtain new structural variants, new properties and, in general, multifunctional materials. Recently in two materials of this group, ((S,S)-DM-EDT-TTF)$_2ClO_4$ and ((R,R)-DM-EDT-TTF)$_2ClO_4$, (DM-EDT-TTF=dimethyl-ethylenedithio-tetrathiafulvalene), a unique effect of magnetochiral anisotropy have been discovered [75].

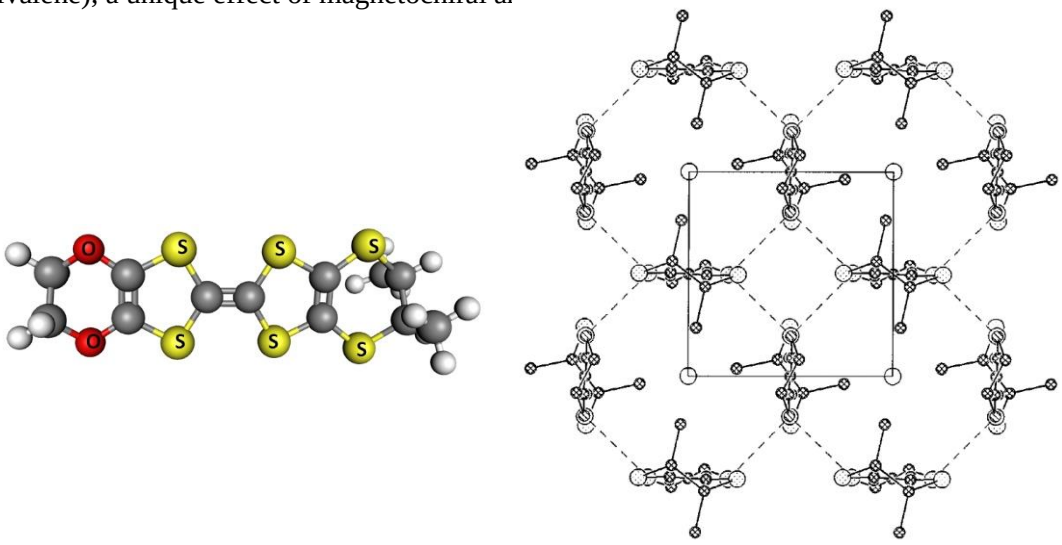

Figure 14: Chiral donor EDO-(*S*,*S*)-DMEDT-TTF molecule (on the left) and conducting layer (on the right) of τ-(EDO-(*S*,*S*)-DMEDT-TTF)$_2$($AuBr_2$)($AuBr_2$)$_y$ (Reprinted with permission from [78]. Copyright 2000 The American Physical Society).

Several materials varying in the structure of the conducting layer, have been investigated. τ-(EDO-(S,S)-DMEDT-TTF)$_2$($AuBr_2$)($AuBr_2$)$_y$, where y ≈ 0.75, crystallizes in the tetragonal system, the so-called τ-phase [76,77]. Donor molecules EDO-(S,S)-DMEDT-TTF are arranged orthogonally in the unit cell and form a network in the conducting plane with short contacts S···S and O···O (Fig. 14). Significant charge transfer occurs between molecules at 90º angle to each other [79]. A characteristic feature of the material is a non-integer value y ≈ 0.75, related with the presence of partially disordered $AuBr_2$ ions between the conducting layers [79]. τ-(EDO-(S,S)-DMEDT-TTF)$_2$($AuBr_2$)($AuBr_2$)$_y$, with y

≈ 0.75 is metallic to low temperatures [79]. Magneto-resistance studies suggested a metal-insulator phase transition of unknown origin below 10 K [80].

The family of chiral salts based on DM-EDT-TTF (Fig. 15(a)), has been recently developed and synthesized by N. Avarvari et al. through controlled introduction of chirality [81]. Utilizing donor molecules of different chirality, three salts containing PF_6 anions were obtained, two based on pure enantiomers (S,S) or (R,R), and a third one containing their racemic mixture. Both pure enantiomer salts, ((S,S)-DM-EDT-TTF)$_2PF_6$ and ((R,R)-DM-EDT-TTF)$_2PF_6$, crystallize in the chiral space group $P2_1$ and are insulators due to the presence of differently charged donor molecules. On the other hand, the racemic (rac-DM-EDT-TTF)$_2PF_6$ salt crystallizing in the centrosymmetric P-1 group, is an organic metal at room temperature and shows a metal-insulator transition at 110 K [81] (Fig. 15(b)). The arrangement of donor molecules in (rac-DM-EDT-TTF)$_2PF_6$ resembles the β-type structure of BEDT-TTF salts, with short contacts between fluorine atoms in the anion layer and ending groups of donor molecules in the conducting layer. The conducting evenly distributed stacks of donor molecules are observed along the (a-b direction) (Fig. 15(c)). These stacks interact with each other, resulting in significantly curved quasi-two-dimensional Fermi surfaces [81].

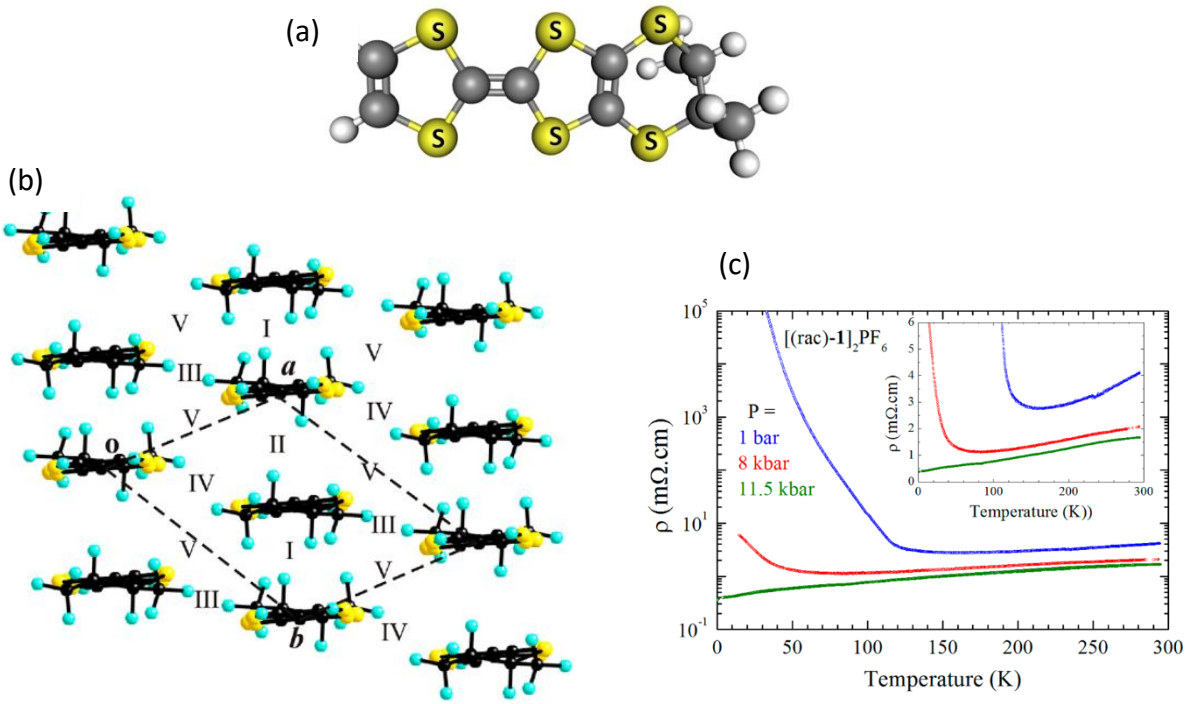

Figure 15: (a) Chiral DM-EDT-TTF donor molecule; (b) conducting layer and (c) temperature and pressure dependence of resistivity of (rac-DM-EDT-TTF)$_2PF_6$ (Reprinted with permission from [81]. Copyright 2013 American Chemical Society).

4. Results

a. Magnetic field dependent vibrational modes in κ-(BEDT-TTF)$_2$X salts

This study was focused on those intramolecular vibrational modes that might be involved in the superconducting to normal state transition in κ-(BEDT-TTF)$_2$X organic superconductors below the critical temperature. In particular, we have looked for the changes in bands that appear in the infrared spectra as a result of electron-intramolecular vibration coupling. Our motivation was related with a persistent discussion, both in the case of organic superconductors [82-84] and high-temperature conductors [85,86], on the possible contribution of the conventional mechanism of electron pairing involving coupling with the lattice to the stabilization of the superconducting state. Such a mechanism was earlier confirmed in the case of superconductors based on fullerene [87]. In the experimental setup magnetic field has been used to switch between superconducting and normal states in the κ-(BEDT-TTF)$_2$X salts that are characterized by critical fields of the order of a few T. The experiment was performed at constant temperature of 4.2 K, much lower than the critical temperature in the superconducting κ-(BEDT-TTF)$_2$X salts. It was important from the point of view of optical spectroscopy, in which we struggle with local heating of the sample. The measurement concept is shown in the diagram in Fig. 16(a).

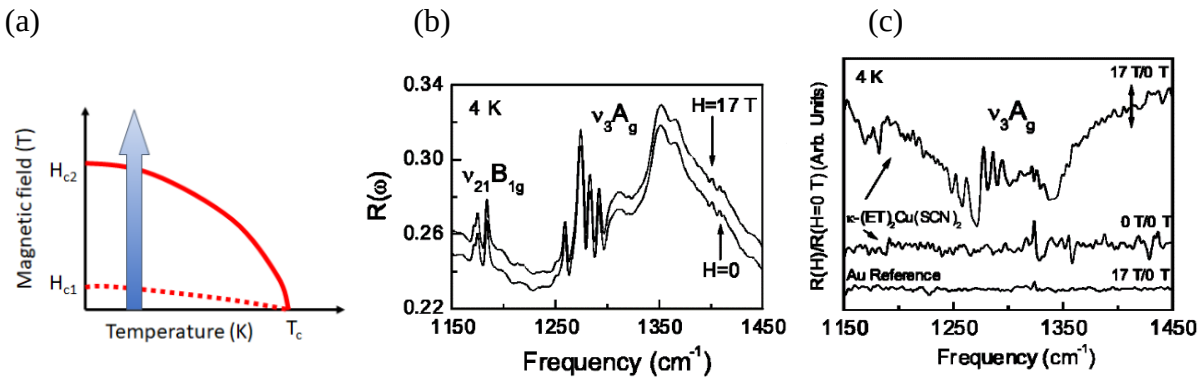

Figure 16: (a) Schematic diagram of the measurement concept. (b) Unpolarized reflectance spectra of κ-(BEDT-TTF)$_2$Cu(SCN)$_2$ (critical field ~ 4.5 T) at 0 and 17 T, in the frequency range of the ν_3 mode characterized by the largest change between the superconducting and normal states (Reprinted with permission from [88]. Copyright 2003 The American Physical Society); c) Reflectance ratio spectra of κ-(BEDT-TTF)$_2$Cu(SCN)$_2$ at 17 T compared with the ratio spectra calculated for the gold reference (Au mirror). The reference ratio spectra measured on the sample before and after the magnetic field sweep (0 T/0 T) reflect the noise level of the measurement. The double arrow indicates a 1% change of the reflectance value (Reprinted with permission from [88]. Copyright 2003 The American Physical Society).

Figure 16(b) shows unpolarized reflectance spectra of κ-(BEDT-TTF)$_2$Cu(SCN)$_2$ measured at the extreme values of magnetic fields, 0 and 17 T, in the frequency range corresponding to the totally symmetric C=C stretching ν_3 mode that is characterized by the largest electron-molecular vibration coupling constant and therefore the most sensitive to phase transitions [88]. Observed modifications of vibrational features under magnetic field are inherently small due to the scale of energy, therefore for the discussion of the results we use the reflectance ratio spectra calculated from the reflectance spectra averaged over multiple measurements for a selected value of magnetic field and a similarly obtained spectra typically measured in zero field. Figure 16(c) shows a clear effect observed for the ν_3 band.

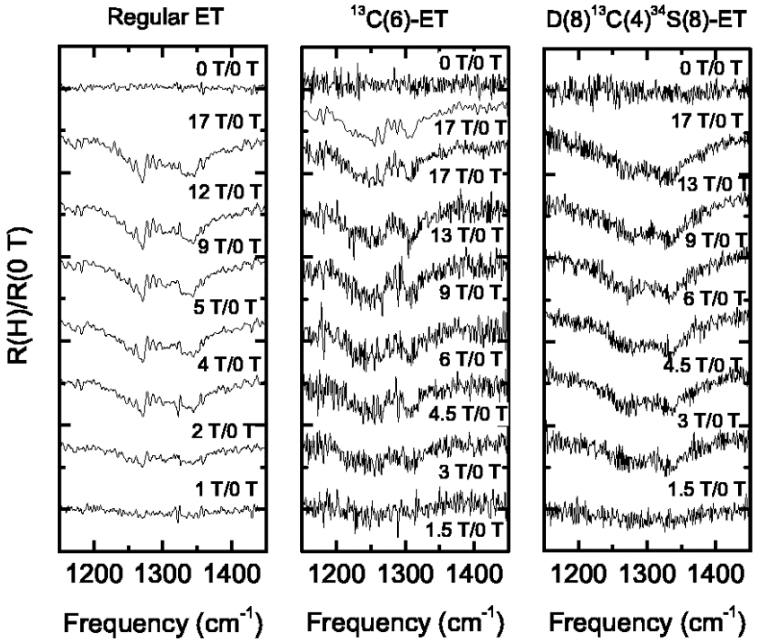

Figure 17: Reflectance ratio spectra R(H)/R(0 T), in the frequency range of ν_3, of regular and isotopically substituted κ-(BEDT-TTF)$_2$Cu(SCN)$_2$ as a function of magnetic field (regular on the left; ^{13}C-substituted sample in the center panel; deuterium, ^{13}C and ^{34}S-substituted sample on the right). The curves are offset for clarity, the top spectrum in each panel is calculated with 0 T results before and after the magnetic field sweep (Reprinted with permission from [90]. Copyright 2003 The American Physical Society).

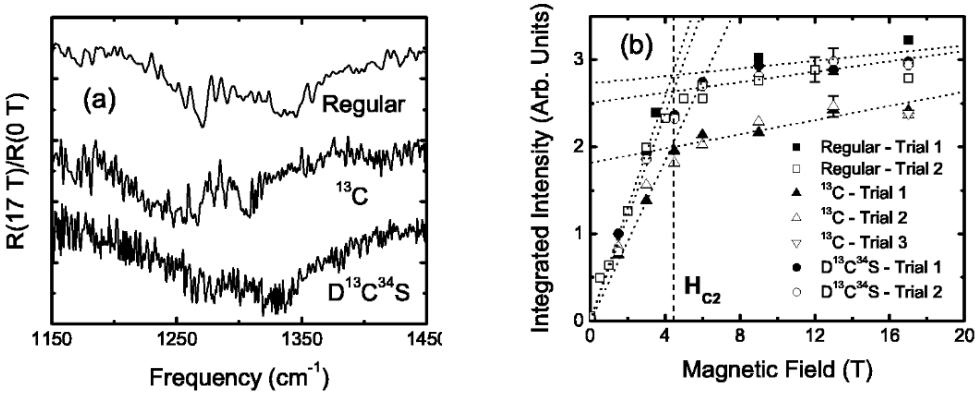

Figure 18: (a) R(17 T)/R(0 T) ratio spectra in the frequency range of ν_3 for the three samples of κ-(BEDT-TTF)$_2$Cu(SCN)$_2$: regular, ^{13}C-substituted, and carbon ^{13}C- and sulfur ^{34}S-substituted. (b) Absolute value of the integrated intensity of the ν_3 feature observed in the ratio spectra (Fig. 18(a)) as a function of applied magnetic field. The vertical dashed line marks the location of the critical field H_{c2} (Reprinted with permission from [90]. Copyright 2003 The American Physical Society).

It is known that the isotope effect can be used to clarify the mechanism of superconductivity [89]. Following this idea, the samples of the κ-(BEDT-TTF)$_2$Cu(SCN)$_2$ superconductor with two variants of isotopic substitutions in BEDT-TTF molecule: 1) carbon ^{13}C, 2) deuterium, carbon ^{13}C and sulfur ^{34}S (Fig. 9) have been investigated under magnetic field [90]. The deuterium/carbon/sulfur substitution is characterized by the critical temperature increased by about 0.2 K in comparison with the salt substituted only with carbon ^{13}C or the regular material [89]. The reflectance ratio spectra of κ-(BEDT-TTF)$_2$Cu(SCN)$_2$ and its isotopically decorated variants in the range of ν_3 are shown in Fig. 17 [90]. The magnetic field induced change in intensity of the ν_3 mode is revealed gradually with the increase of the magnetic field in case of all the examined samples, with the ν_3 profiles slightly differing in shape among different samples, in connection with isotopic substitutions [90]. To quantify the observed modifications

of the reflectance spectra, the intensity of the effect in the ratio spectra has been calculated as the area with respect to the horizontal base line over the frequency range shown in Fig. 18(a). The results of the calculations as a function of magnetic field demonstrate a correlation between the observed effect and the critical field H_{c2} ~ 4.5 T (Fig. 18(b)) [90]. Below H_{c2} we observe a clear linear dependence of intensity on the magnetic field. Above H_{c2} the effect is partly saturated. In our study we have not observed any differences that could be ascribed to the isotopic effect with respect to the critical field.

Optical measurements under magnetic field were also performed for two other κ-phase salts, the superconductor κ-BEDT-TTF)$_2$Cu[N(CN)$_2$]Br [9,91], characterized by the highest critical temperature T_c = 11.6 K and the largest critical field H_{c2} ~ 6.5 T in this group of materials, and the antiferromagnetic insulator κ-(BEDT-TTF)$_2$Cu[N(CN)$_2$]Cl [58,92]. The aim of this study was to confirm the correlation between the effect observed earlier for the EMV-activated vibrational bands in κ-(BEDT-TTF)$_2$Cu(SCN)$_2$, with critical field H_{c2} and thus the superconducting state. Figure 19 shows R(H)/R(0 T) reflectance ratio spectra of κ-(BEDT-TTF)$_2$Cu[N(CN)$_2$]Br in the range of several totally symmetric BEDT-TTF vibrations activated in IR spectra by coupling with charge transfer: ν_4 (Ag) (left), ν_{10} (Ag) (middle) and ν_{13} (Ag) (right) [93]; here the vibrational modes are described in a more realistic C_{2h} symmetry [94], in which the stretching C=C vibration most strongly EMV-coupled is denoted as ν_4 (ν_3 in D_{2h}). Changes as a function of magnetic field are observed in all the vibrational modes; it is suggested that they apply to all vibrations activated as a result of EMV coupling.

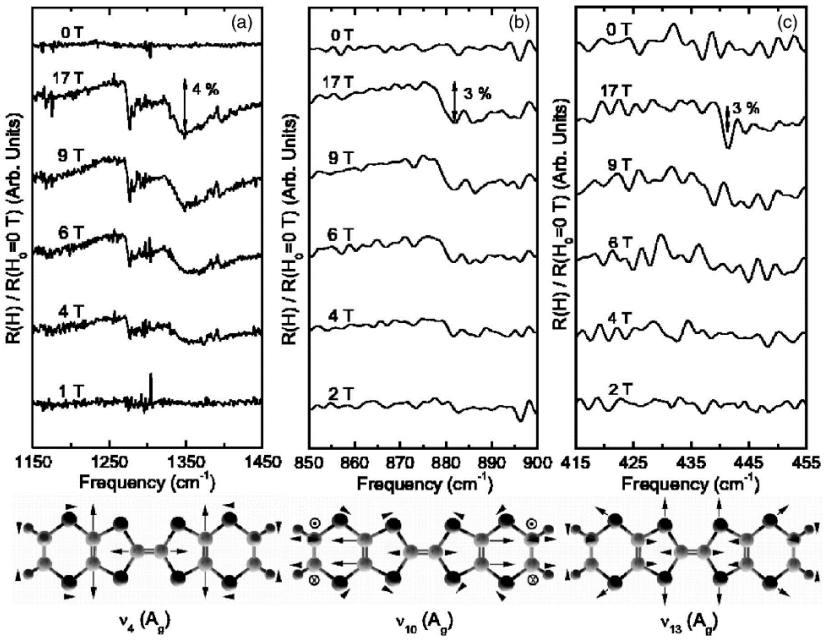

Figure 19: Reflectance ratio spectra R(H)/R(0 T) of κ-(BEDT-TTF)$_2$Cu[N(CN)$_2$]Br in the frequency range of the selected vibrational BEDT-TTF modes as a function of magnetic field: (a) ν_4 (A_g) (corresponds to the C=C stretching ν_3 mode in the D_{2h} symmetry). (b) ν_{10} (A_g), and (c) ν_{13} (A_g); corresponding mode patterns in the C_{2h} symmetry are schematically shown below. The curves are offset for clarity, the top spectrum in each panel is calculated with 0 T results before and after the magnetic field sweep (Reprinted with permission from [93]. Copyright 2005 The American Physical Society).

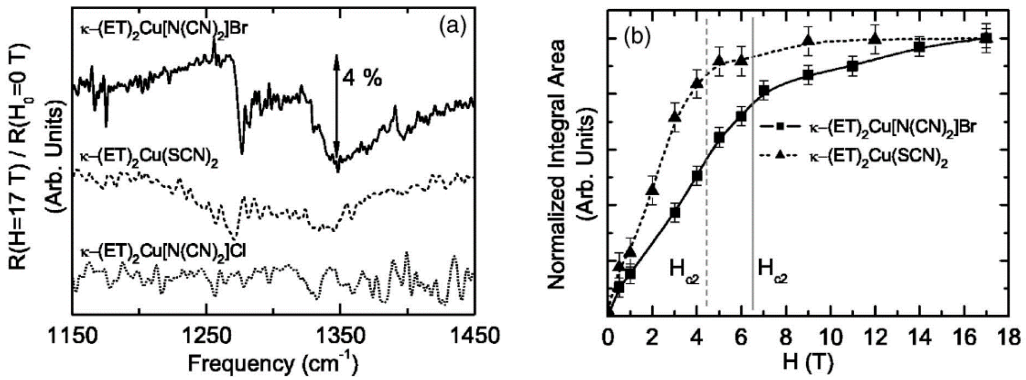

Figure 20: (a) Comparison of the reflectance ratio spectra R(17T)/R(0T) in the frequency range of the totally symmetric C=C stretching ν_4 mode (ν_3 in D_{2h} symmetry) for κ-(BEDT-TTF)$_2$Cu(SCN)$_2$, κ-(BEDT-TTF)$_2$ Cu[N(CN)$_2$]Br and κ-(BEDT-TTF)$_2$Cu[N(CN)$_2$]Cl. (b) Normalized integral area of the changes in the reflectance ratio shown in panel (a) for for κ-(BEDT-TTF)$_2$Cu(SCN)$_2$ and κ-(BEDT-TTF)$_2$ Cu[N(CN)$_2$]Br superconductors as a function of applied magnetic field, with dashed and solid vertical lines indicating H_{c2} values, respectively. Lines connecting the data points are guide for an eye. Estimated error bars are also shown (Reprinted with permission from [93]. Copyright 2005 The American Physical Society).

Figure 20(a) displays a comparison of the R(17T)/R(0T) spectra for κ-(BEDT-TTF)$_2$Cu(SCN)$_2$, κ-(BEDT-TTF)$_2$Cu[N(CN)$_2$]Br, and κ-(BEDT-TTF)$_2$Cu[N(CN)$_2$]Cl [93]. In case of the κ-(BEDT-TTF)$_2$[N(CN)$_2$]Cl salt, which is not superconducting in the measurement conditions, there are no characteristic changes of vibrational bands in the magnetic field, as expected. Thus, we suggest that the effect observed in reflectance spectra under magnetic field for the other materials is characteristic for the superconducting state. The intensity of the effect as a function of magnetic field shows a clear correlation with the critical field value, which is about 6.5 T for κ-(BEDT-TTF)$_2$Cu[N(CN)$_2$]Br salt (Fig. 20(b)) [93].

In the summary of the investigations of intramolecular vibrational modes in the superconducting κ-(BEDT-TTF)$_2$X salts under magnetic field it should be emphasized that there is no reason to attribute a significant role in the transition to a superconducting state to the EMV coupling [45]. The observed effect is related to the change of the electronic structure, which is in this way revealed.

b. Charge localization in the β′′- and β′-phase BEDT-TTF salts

i. β′′-(BEDT-TTF)$_2$RCH$_2$SO$_3$ (R = SF$_5$, CF$_3$) salts: charge ordering

β′′-(BEDT-TTF)$_2$SF$_5$CH$_2$SO$_3$ and β′′-(BEDT-TTF)$_2$SF$_5$CH$_2$SO$_3$ salts [61,65], display typical layered architecture, with BEDT-TTF molecules inclined at about 60° angle with respect to the stacking axis. There are two crystallographically independent BEDT-TTF molecules A and B in the conducting layer, which form ribbons connected by close contacts (Fig. 12(a)). The anions in these materials are dimerized due to the presence of hydrogen bonding (Fig. 12(b)). Both materials exhibit semiconducting properties down to the low temperature and significant charge disproportionation between molecules A and B, as suggested based on the bond lengths analysis [48,65]. Thus, the infrared reflectance and Raman spectra of the β′′-(BEDT-TTF)$_2$RCH$_2$SO$_3$ salts has been investigated in order to provide more information on the origin of charge localization [65].

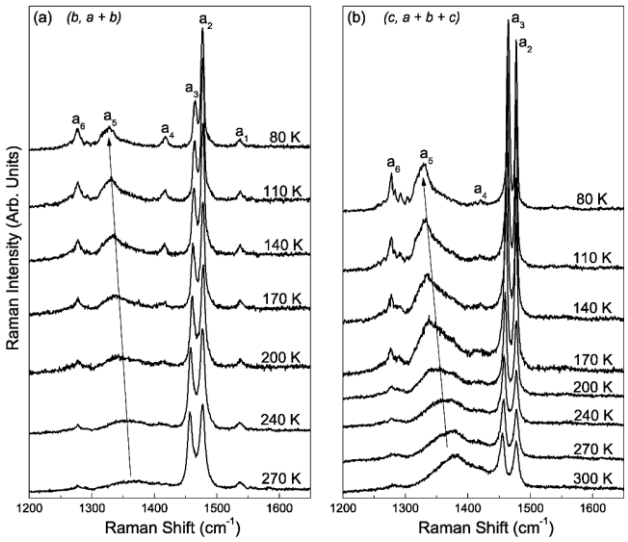

Figure 21: Raman spectra of β′′-(BEDT-TTF)$_2$CF$_3$CH$_2$SO$_3$ along the *b* (a) and *c* (b) axes (Reprinted with permission from [65]. Copyright 2009 Royal Society of Chemistry).

Figure 21 shows Raman spectra of β′′-(BEDT-TTF)$_2$CF$_3$CH$_2$SO$_3$ as a function of temperature. The presence of the two ν_2 mode components a_1 and a_2 centered at 1478 cm^{-1} and 1538 cm^{-1}, respectively, indicates that differently charged BEDT-TTF molecules are present in the material over the entire temperature range. The charges estimated from the ν_2 mode components are 0.2*e* and 0.8*e*, which is consistent with the values calculated from the bond lengths. A strong band marked as a_5, which shifts to lower frequencies as temperature decreases, is another prominent feature observed in the Raman spectra. The band is attributed to a component of the ν_3 mode that is strongly disturbed by EMV coupling and usually activated in the infrared spectra. Such observation indicates the existence of asymmetrically charged BEDT-TTF dimers in the structure [95].

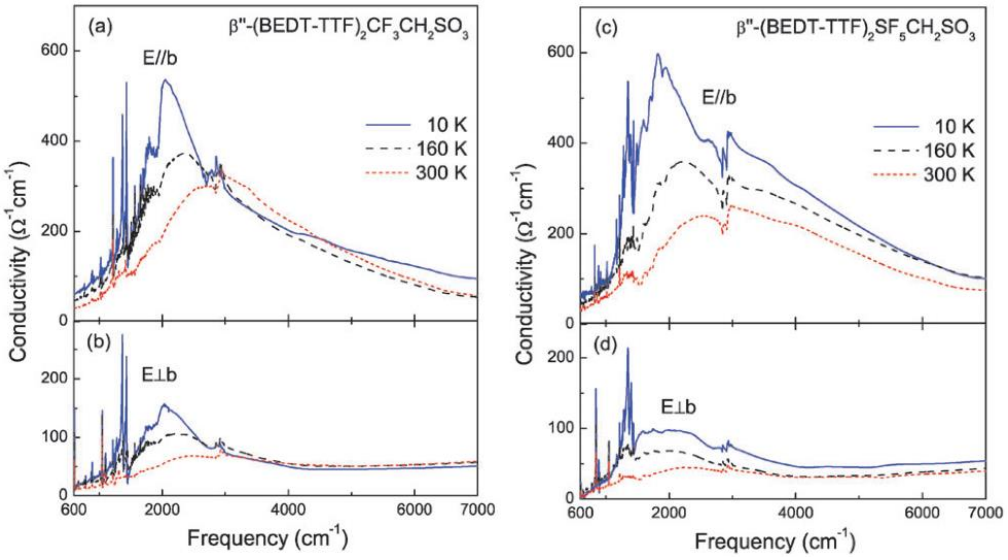

Figure 22: Polarized optical conductivity spectra of β′′-(BEDT-TTF)$_2$CF$_3$CH$_2$SO$_3$ (a,b) and β′′-(BEDT-TTF)$_2$SF$_5$ CH$_2$SO$_3$ (c,d) at selected temperatures (Reprinted with permission from [65]. Copyright 2009 Royal Society of Chemistry).

Selected optical conductivity spectra of β′′-(BEDT-TTF)$_2$SF$_5$CH$_2$SO$_3$ and β′′-(BEDT-TTF)$_2$SF$_5$CH$_2$SO$_3$ polarized in two principal directions in the conducting plane are shown in Figure 22. They indicate the two-dimensional character of the interactions in the conducting plane as expected. In

both materials a wide, asymmetrical electronic band at ≈2000 cm^{-1} is observed. It increases its intensity during the temperature decrease; at the same time the low frequency edge becomes sharp and asymmetric, which indicates the presence of an energy gap. Vibrational features observed in the spectra of both materials below 1600 cm^{-1} are characterized by strong temperature dependence (Fig. 23). At room temperature few weak bands are observed, related to infrared-active anion modes, but with lowering the temperature strong BEDT-TTF modes activated as a result of EMV coupling (vibronic bands) are gradually emerging in the spectra. In particular, there are two characteristic ν_3 mode components, which indicate both the presence of differently charged donor molecules in the material and lowering the symmetry of the system related with dimerization (Fig. 23). This kind of vibrational response may also indicate the presence of symmetrical tetrameters that consist of two asymmetrical dimers [96]. Although dimerization in β′′-(BEDT-TTF)$_2$RCH$_2$SO$_3$ salts is present in the anionic layer in the whole temperature range, it is revealed in the optical conductivity spectra of the conducting layer below about 150 K, the temperature of ordering of the terminal ethylene groups of BEDT-TTF. Therefore, we suggest that dimerization in the β′′-(BEDT-TTF)$_2$CF$_3$CH$_2$SO$_3$ and β′′-(BEDT-TTF)$_2$SF$_5$CH$_2$SO$_3$ salts occurs with the participation of hydrogen bonding between anions, and between anions and conducting BEDT-TTF layer [65].

Figure 23 (e) displays the room temperature optical conductivity spectrum of β′′-(BEDT-TTF)$_2$SF$_5$CH$_2$SO$_3$ measured in a polarization perpendicular to the conducting plane, which allows to examine ν_{27} feature. In our case, the splitting of the ν_{27} mode components enabled the determination of the charges localized on the molecules A and B, to be 0.2*e* and 0.7*e* respectively [65]. In fact, a checkerboard CO pattern has been recently confirmed in this material [97].

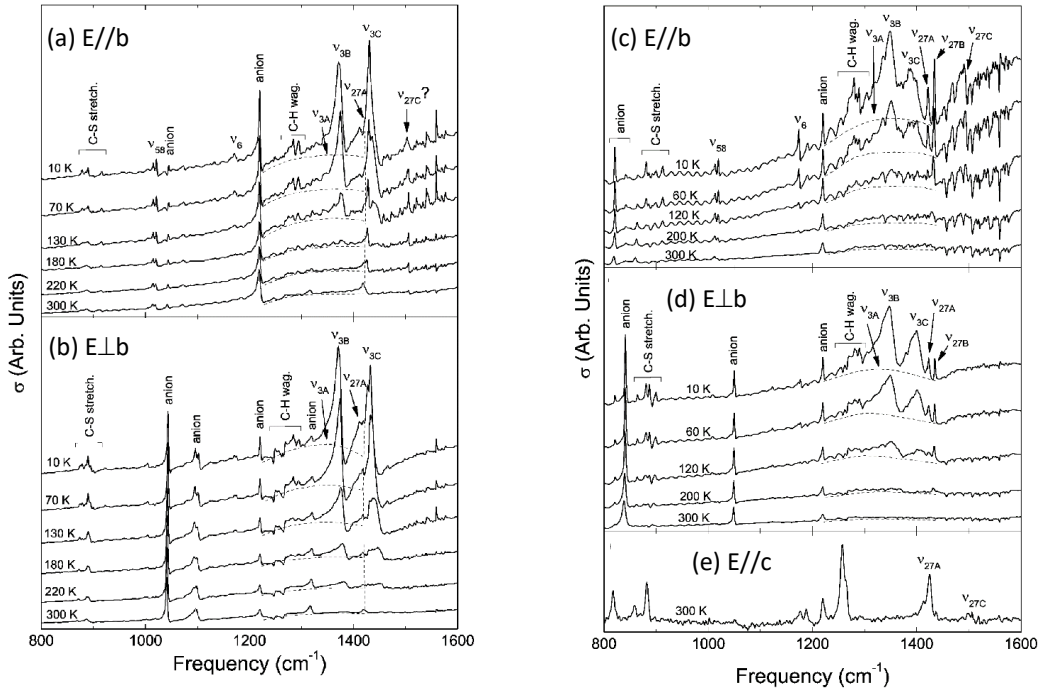

Figure 23: Close-up view of the optical conductivity spectra in the vibrational frequency range of β′′-(BEDT-TTF)$_2$CF$_3$CH$_2$SO$_3$ ((a), (b)) and β′′-(BEDT-TTF)$_2$SF$_5$CH$_2$SO$_3$ ((c), (d)) as a function of temperature; spectra are offset for clarity. (e) room temperature optical conductivity spectrum of β′′-(BEDT-TTF)$_2$SF$_5$CH$_2$SO$_3$ in the interplane direction (Reprinted with permission from [65]. Copyright 2009 Royal Society of Chemistry).

ii. β′′-(BEDT-TTF)$_4$[(H$_3$O)Fe(C$_2$O$_4$)$_3$]·Y salts: charge fluctuations

The β′′-(BEDT-TTF)$_4$[(H$_3$O)M(C$_2$O$_4$)$_3$]·Y (M=magnetic ion, Y = solvent molecule) salts are known to display heterogeneous distribution of charge on the border of superconducting, metallic and insulating states [98]. Of interest here are salts with M=Fe and benzonitrile, bromobenzene and fluorobenzene solvent molecules (Fig. 13). β′′-(BEDT-TTF)$_4$[(H$_3$O)Fe(C$_2$O$_4$)$_3$]·C$_6$H$_5$Br (abbreviated β′′-1) shows structural phase transition at 160-200 K and superconductivity near 4 K [69]. Studies by tunneling spectroscopy suggest the presence of a mixed superconducting-insulating state at low temperature in this material [99]. The other two materials, containing mixtures of benzonitrile with bromobenzene and fluorobenzene: β′′-(BEDT-TTF)$_4$[(H$_3$O)Fe(C$_2$O$_4$)$_3$]·(C$_6$H$_5$CN)$_{0.17}$ (C$_6$H$_5$Br)$_{0.83}$ (β′′-2) and β′′-(BEDT-TTF)$_4$[(H$_3$O)Fe(C$_2$O$_4$)$_3$] -(C$_6$H$_5$CN)$_{0.4}$(C$_6$H$_5$F)$_{0.6}$ (β′′-3), display superconductivity and structural phase transition in similar temperature ranges [70,74]. The α-"pseudo-κ"-(BEDT-TTF)$_4$[(H$_3$O)Fe(C$_2$O$_4$)$_3$]·C$_6$H$_4$Br$_2$ (α-κ) salt, which exhibits metallic properties in the whole temperature range [100], has been used as a reference.

The reflectance spectra of β′′-1, β′′-2 and β′′-3 salts at room temperature are similar, characteristic for organic metals (Fig. 24). The charge transfer electronic band is centered in the optical conductivity spectra at ≈2500 cm^{-1} in all materials, as revealed with the help of the Drude-Lorentz model (the arrow in the inserts) [101].

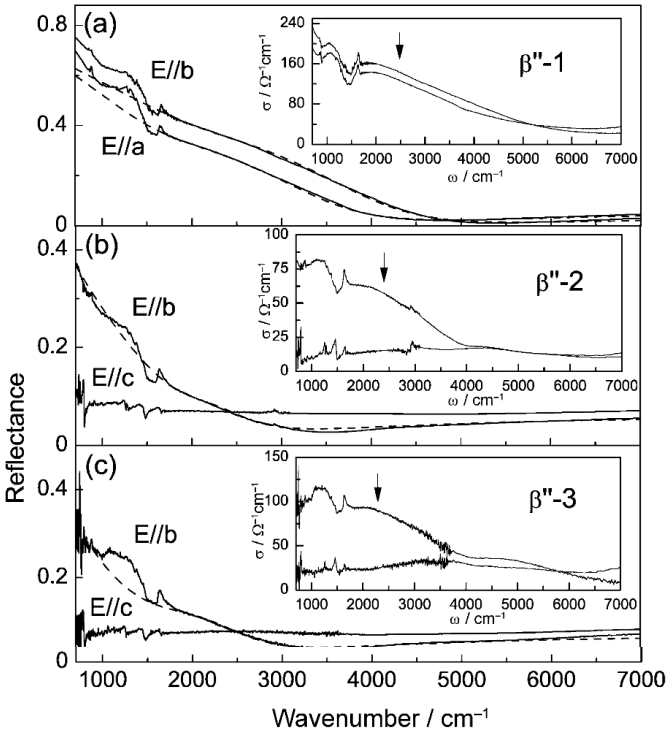

Figure 24: Polarized reflectance and optical conductivity spectra at room temperature for β′′-(BEDT-TTF)$_4$[(H$_3$O)Fe(C$_2$O$_4$)$_3$]·Y salts designated as β′′-1, β′′-2, β′′-3 (see text). The arrows in inserts show the position of the middle infrared electronic band, as fitted with the Drude-Lorentz model (Reprinted with permission from [101]. Copyright 2013 Wiley-VCH Verlag GmbH & Co. KGaA, Weinheim).

In the search for effects related to charge fluctuations, Raman investigations in the frequency range of the charge-sensitive ν_2 mode of BEDT-TTF molecule have been performed. Figure 25 (b,c) shows the Raman spectra measured for β′′-1 and β′′-2 at selected temperatures. At the same time, the optical conductivity spectra of the β′′-2 and β′′-3 salts polarized in the direction perpendicular to the conducting layer, display charge-sensitive ν_{27} mode that is known to be the best probe of charge localized on BEDT-TTF [101]. The β′′ salts are characterized with a quarter filled conducting band and an average charge

of 0.5*e* per donor molecule. On the other hand, they are poorly dimerized, which often correlates with the presence of charge fluctuations. The bands of relevant vibrations characteristic for molecules with charge 0.5e are marked as ν_{2B} in the Raman spectra and ν_{27B} in the optical conductivity spectra (Fig. 25). Note that both in Raman and IR spectra, these bands are significantly broadened, suggesting the presence of charge fluctuations in the investigated β′′ salts. Thus, considering the width of the ν_2 mode of about 5 cm^{-1} at low temperature we estimate the amplitude of charge fluctuation as $\Delta\rho = 0.04$ for β′′-1 and β′′-2 salts [96,101].

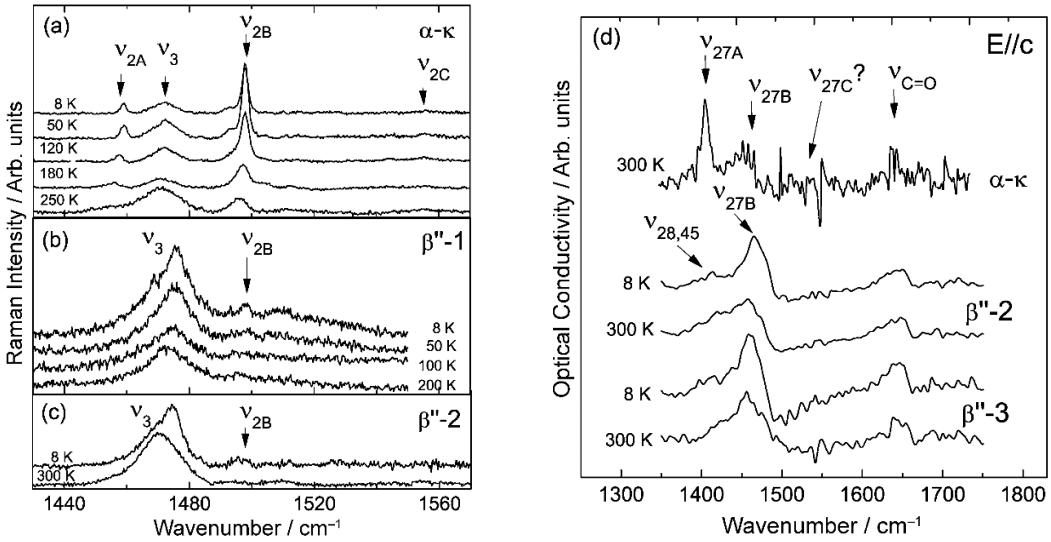

Figure 25: Raman (a-c) and IR (d) spectra of the β′′-(BEDT-TTF)$_4$[$(H_3O)Fe(C_2O_4)_3$]·Y salts β′′-1 (b), β′′-2 (c,d), β′′-3 (d), together with the reference α-κ insulating material (a,d), in the frequency range of charge-sensitive ν_2 and ν_{27} C=C stretching modes of BEDT-TTF (Reprinted with permission from [101]. Copyright 2013 Wiley-VCH Verlag GmbH & Co. KGaA, Weinheim).

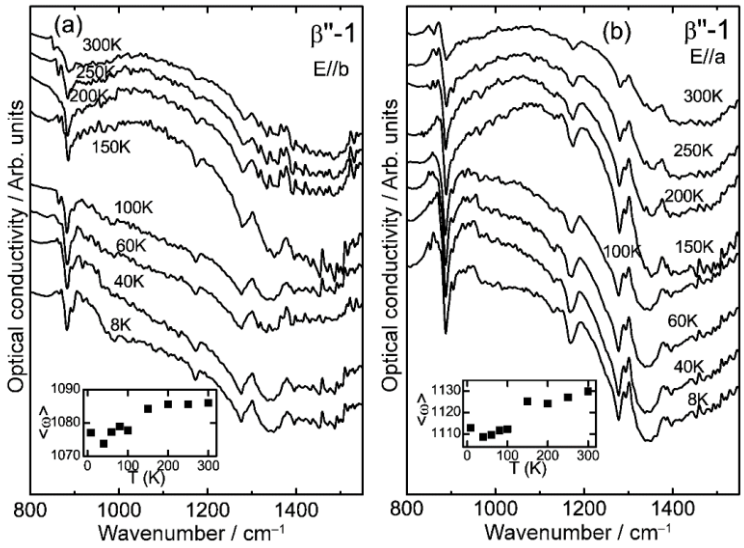

Figure 26: Polarized optical conductivity spectra of β′′-(BEDT-TTF)$_4$[$(H_3O)Fe(C_2O_4)_3$]·C_6H_5Br, in the frequency range of EMV-activated ν_3 mode. Inserts show the shift of the center of spectral density <ω> as a function of temperature (Reprinted with permission from [101]. Copyright 2013 Wiley-VCH Verlag GmbH & Co. KGaA, Weinheim).

A sharp anomaly in the shape of the optical conductivity spectra is observed between 100 and 150 K for the β′′-1 salt, in the frequency range of the strong ν_3 stretching C=C mode activated by EMV coupling (Fig. 26). The center of spectral weight calculated for this broad ν_3 feature displays a significant

downshift in both principal polarization directions on lowering the temperature between 150 and 100 K (inserts in Fig. 26). Such a redistribution of spectral weight points to a change in electronic charge transfer excitation and suggests a transition to a mixed metal/insulator phase in β′′-1 in this temperature range [101].

iii. β′-(BEDT-TTF)$_2$CF$_3$CF$_2$SO$_3$ dimer Mott insulator: charge ordering and lattice distortion

β′-(BEDT-TTF)$_2$CF$_3$CF$_2$SO$_3$ is characterized by a dimerized one-dimensional stacking of BEDT-TTF molecules, with two equivalent conducting layers in the unit cell (Fig. 12(c,d)). Electronic band structure calculations confirm a predominantly one-dimensional character of the material, with conducting stacks running along **b-a** direction, which is diagonal in the conducting donor plane [64].

Figure 27 shows the infrared reflectance and optical conductivity spectra polarized in the two principal polarization directions at selected temperatures. Such an anisotropic response with mostly conducting **b-a** direction is expected in case of a dimerized β′ structure. The overall shape of the optical conductivity spectra can be described as a dimer-Mott insulator in the whole temperature range, with the Hubbard component centered at ≈2700 cm^{-1} and the dimer band at ≈3600 cm^{-1}. A significant increase of spectral weight on lowering the temperature from 300 to 10 K is observed only in the vicinity of the maximum of the Hubbard band at 2700 cm^{-1} in the stack direction (Fig. 27(c)).

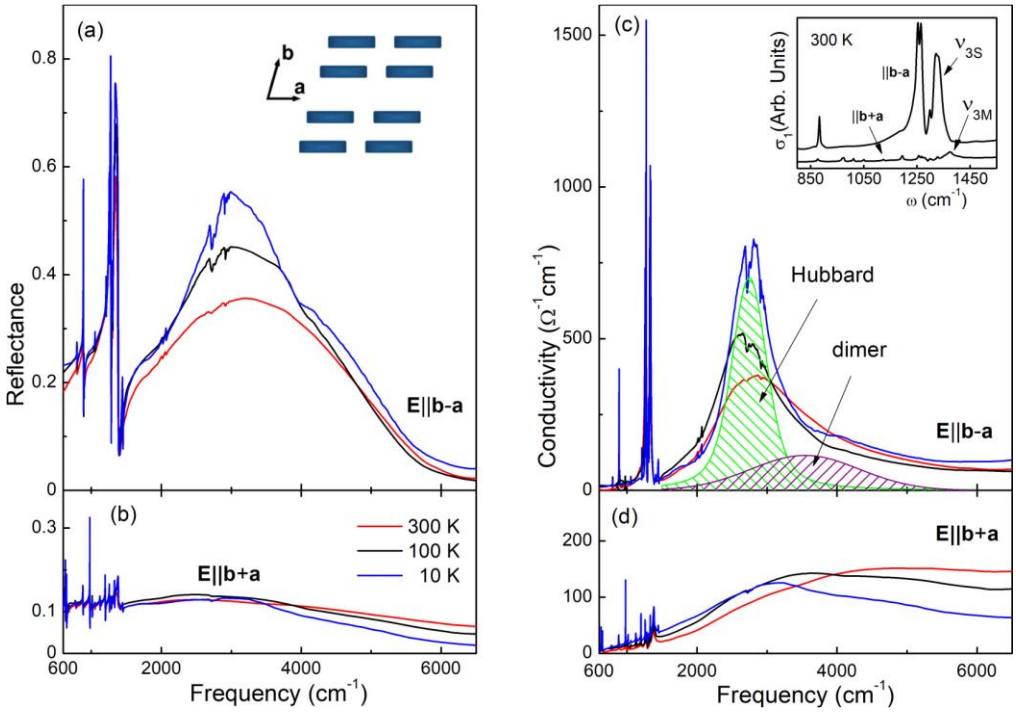

Figure 27: Polarized reflectance and optical conductivity spectra of β′-(BEDT-TTF)$_2$CF$_3$CF$_2$SO$_3$ for E//b-a (a, c) and E//b+a (b, d), at selected temperatures T = 300 K, 100 K, and 10 K. Two electronic band components, Hubbard and dimer, are marked in panel (c).The insets display the simplified structure of the conducting layer (a) and a close-up view of the 300 K optical conductivity in the vibrational range (c) (Reprinted with permission from [64]. Copyright 2020 American Physical Society).

Raman spectra of β′-(BEDT-TTF)$_2$CF$_3$CF$_2$SO$_3$ in the frequency range of charge-sensitive C=C stretching BEDT-TTF modes have been measured in order to explore the possibility of charge-ordered

states. Temperature dependence of the Raman spectra recorded for two samples is shown in Fig. 28 (a,b) [64]. We focus our attention on the v_2 and v_{27} vibrations that allow estimation of charge localized on donor molecule. A clear splitting of these features into two components is observed below ≈30 K (Fig. 28 (c)). While single bands above 30 K correspond to the charge ≈0.5*e*, the frequency difference of two components below 30 K is used to estimate charge disproportionation in the CO state. Here, both the v_2 and v_{27} splitting suggest the charge disproportionation of ≈0.1*e*. Considering the specific structure with two equivalent conducting layers, the Raman spectra provide evidence for the low-temperature interlayer CO state [64].

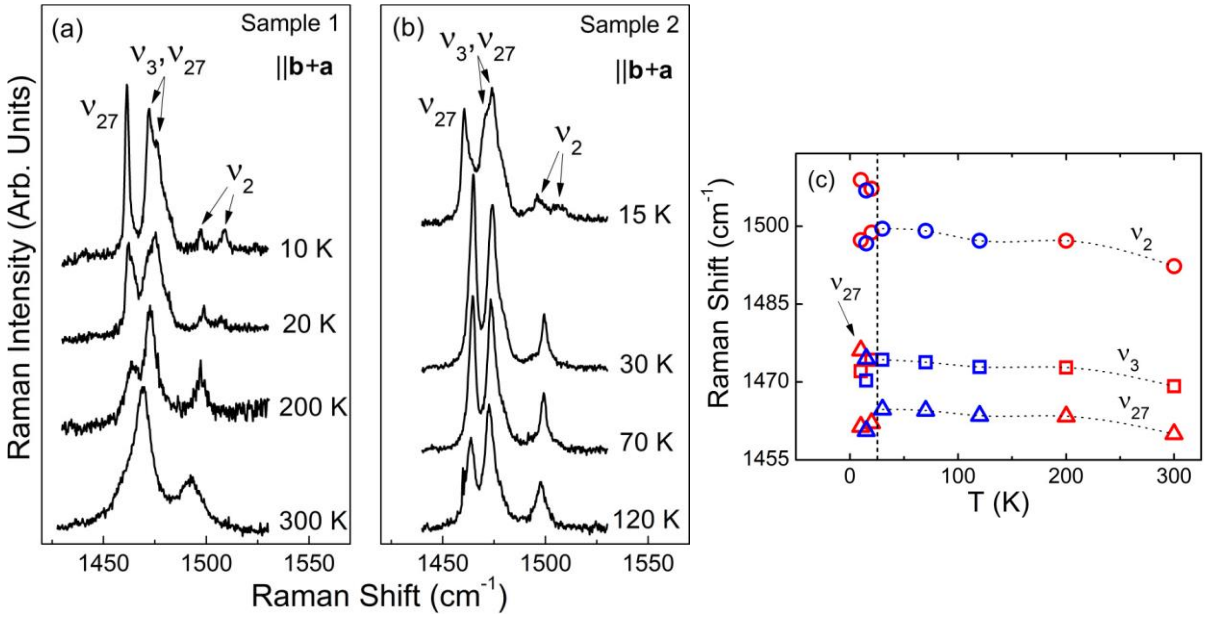

Figure 28: (a,b) Raman spectra of β′-(BEDT-TTF)$_2$CF$_3$CF$_2$SO$_3$ for selected temperatures; spectra are shifted for clarity. Panel (c) displays the Raman shift of the v_{27} (Δ), v_2 (O), and v_3 (□) mode components, as observed in the spectra of sample 1 (red color) and sample 2 (blue). The dashed line marks the approximate splitting temperature of the *v*2 mode is observed. Lines between data points are intended to guide the eye (Reprinted with permission from [64]. Copyright 2020 American Physical Society).

The onset of the charge-ordered phase in β′-(BEDT-TTF)$_2$CF$_3$CF$_2$SO$_3$ is accompanied by lattice distortion, as exemplified by clear splitting of the v_3 mode in optical conductivity spectra into altogether three components at 1446, 1383 and 1330 cm^{-1} below about 30 K (Fig. 29 (a,b)). Considering another v_3 mode observed at 1472 cm^{-1} in Raman spectra, there are as much as four v_3 components identified at low temperature, suggesting a symmetry lowering.

This significant lattice distortion in β′-(BEDT-TTF)$_2$CF$_3$CF$_2$SO$_3$ involves modification of hydrogen bonding-type interaction between terminal ethylene groups of donor molecules and the $CF_3CF_2SO_3^-$ anions. When lowering the temperature between 25 and 20 K, in the optical conductivity spectra in the **b-a** direction we observe a remarkable redshift of the v_1 mode, the C-H symmetric stretching of the ethylene groups, indicating C-H bond lengthening (Fig. 29(c)). The cation-anion interactions are considered to stabilize the CO state in some dimerized BEDT-TTF salts [102,103]. In case of β′-(BEDT-TTF)$_2$CF$_3$CF$_2$SO$_3$ we suggest that this is the CO transition that results in modification of the interactions at the cation-anion interface.

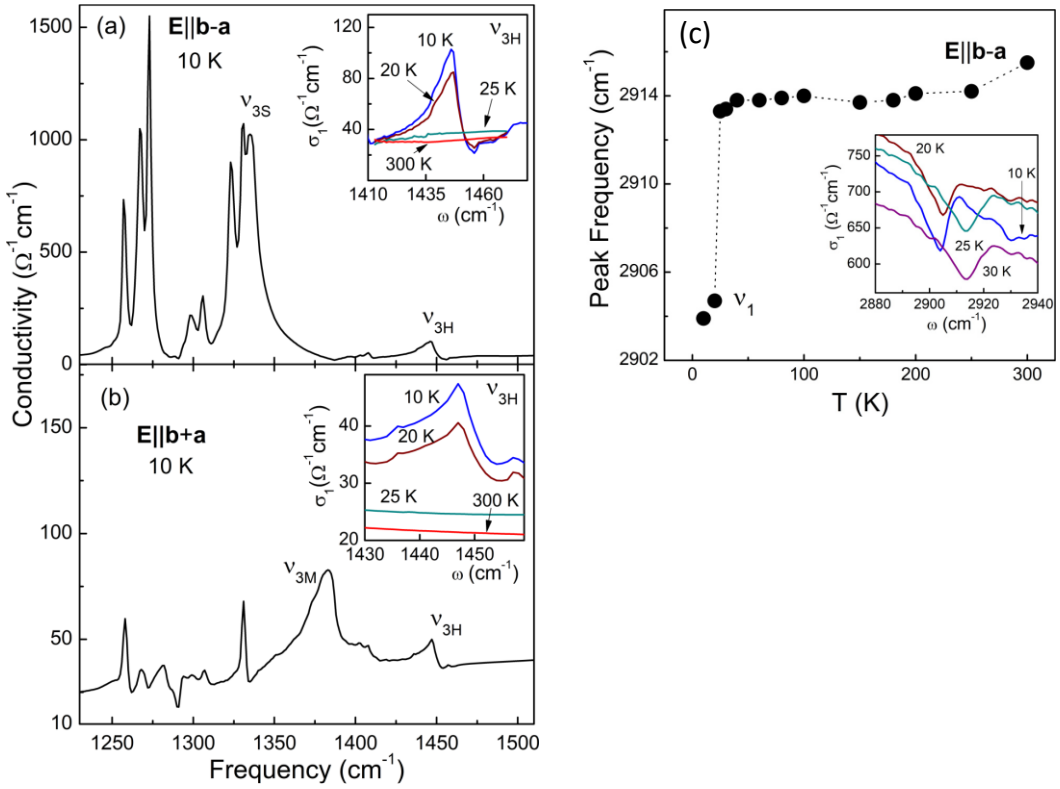

Figure 29: Optical conductivity spectra of β′-(BEDT-TTF)$_2$CF$_3$CF$_2$SO$_3$ at 10 K, in the frequency range of the electron-molecular vibration-activated ν_3 mode for E//b-a (a) and E//b+a (b); insets display close-up views of the temperature dependence of the ν_{3H} mode component at1446 cm^{-1} that appears in both spectra below 30 K. (c) The ν_1 vibrational BEDT-TTF mode observed in optical conductivity spectra in **b-a** direction; inset shows optical conductivity spectra at 10, 20, 25, and 30 K in this frequency range (Reprinted with permission from [64]. Copyright 2020 American Physical Society).

c. Charge localization in the salts with chiral donor molecules

i. Charge localization in τ-(EDO-(S,S)-DMEDT-TTF)$_2$(AuBr$_2$)(AuBr$_2$)$_y$

Investigations of the reflectance spectra of τ-(EDO-(S,S)-DMEDT-TTF)$_2$(AuBr$_2$)(AuBr$_2$)$_y$ with y≈0.75, were aimed at understanding the low temperature charge localization in this organic metal based on unsymmetrical donor molecule, as observed in the studies of direct current conductivity [79] and magnetoresistance [80]. The specific structure of the material allowed measurements using unpolarized light because the polarized reflectance measured from the conducting plane do not display dependence on polarization. The experimental reflectance spectra and optical conductivity spectra calculated using Kramers-Kronig's analysis are presented in Figure 30 [80]. Reflectance spectra are characteristic for organic metal, with no clear plasma edge (Fig. 30 (a)). In the room temperature optical conductivity spectrum two electronic bands at frequencies ≈1000 cm^{-1} and 5500 cm^{-1} are observed. When lowering the temperature from 300 K down to 10 K, the very wide 1000 cm^{-1} band gradually displays splitting into two components, 350 and 1100 cm^{-1}. The observed electronic excitations are discussed based on the Hubbard model [37], which allows to connect the splitting of the electronic band at 1000 cm^{-1} with the charge localization [80]. Indeed, a similar effect of electronic localization related with the band

splitting at low frequency was experimentally observed and theoretically studied in a model dimer Mott insulator [104].

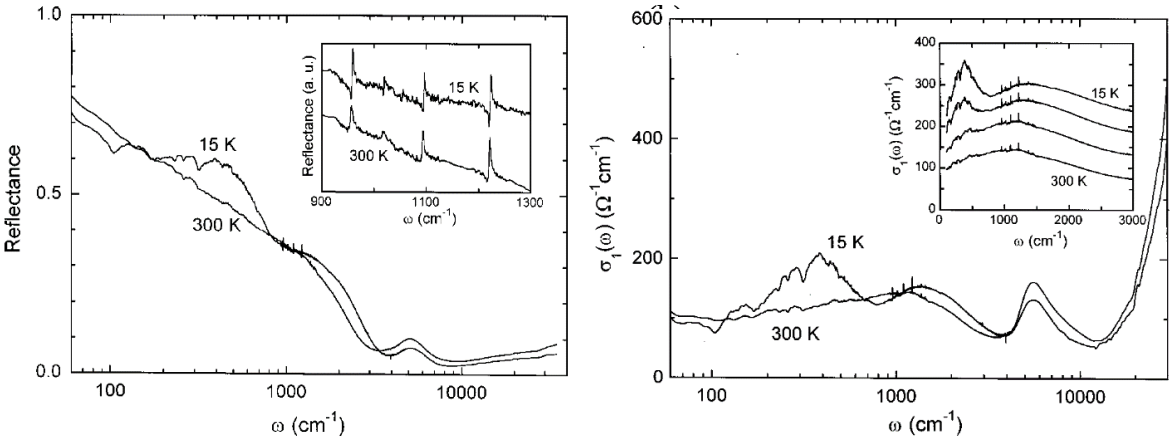

Figure 30: Reflectance (a) and optical conductivity spectra (b) of τ-(EDO-(S,S)-DMEDT-TTF)$_2$(AuBr$_2$)(AuBr$_2$)$_y$ as a function of temperature (Reprinted with permission from [78]. Copyright 2000 The American Physical Society).

ii. Chiral DM-EDT-TTF salts: charge fluctuations

The family of chiral DM-EDT-TTF-based salts of interest here is a complete series including enantiopure ((S,S)-DM-EDT-TTF)$_2$PF$_6$ and ((R,R)-DM-EDT-TTF)$_2$PF$_6$ phases together with the racemic (rac-DM-EDT-TTF)$_2$PF$_6$ that is characterized by weakly dimerized structure of the conducting layer related with the possible presence of the charge-ordered states.

The DM-EDT-TTF molecule is an asymmetrical chiral derivative of tetrathiafulvalene, with three double C=C bonds. Similarly, to BEDT-TTF, the C=C stretching vibrations (Fig. 31) display frequency dependence on charge. Thus, in order to determine the charge distribution in the ((S,S)-DM-EDT-TTF)$_2$PF$_6$, ((R,R)-DM-EDT-TTF)$_2$PF$_6$ and (rac-DM-EDT-TTF)$_2$PF$_6$ salts, we investigated Raman spectra in the frequency range of charge-sensitive C=C stretching modes of DM-EDT-TTF, both experimentally and theoretically using Density Functional Theory (DFT) methods [81]. Results of measurements and calculations are presented in Figure 31. Based on the observed and theoretical frequencies of the bands corresponding to the ν_2 mode (see Fig. 31 for mode pattern) it was found that both salts with the enantiopure donor molecules are charge-ordered insulators in the whole temperature range. On the other hand, in the Raman spectra of racemic (rac-DM-EDT-TTF)$_2$PF$_6$ salt a single broadened ν_2 band is observed in the position corresponding to the charge 0.5e [81].

In the further study of (rac-DM-EDT-TTF)$_2$PF$_6$ that was focused on the 100 K metal-insulator phase transition [81], we investigated variable temperature infrared reflectance as well as Raman spectra for several excitation lines. The polarized reflectance and optical conductivity spectra are shown in Figure 32 [105]. Infrared response is characteristic for quasi-one-dimensional organic metal, in agreement with the transfer integrals (right panel in Fig. 32), as calculated on the basis of the structural parameters [81]. The shape of the optical conductivity spectra and their strong temperature dependence indicate that the material can be regarded as dimer-Mott insulator at low temperature, weakly dimerized along the columns of the donor molecules and strongly dimerized in the perpendicular direction, with the Hubbard band at ≈1100 cm^{-1} in both the principal polarization directions. With lowering the temperature through

the 110 K phase transition, a strong feature related with the stretching ν3 mode of DM-EDT-TTF activated due to electron-molecular vibration coupling appears in the optical conductivity spectra polarized in the stack **a-b** direction at ≈1300 cm^{-1} (Fig. 33a).

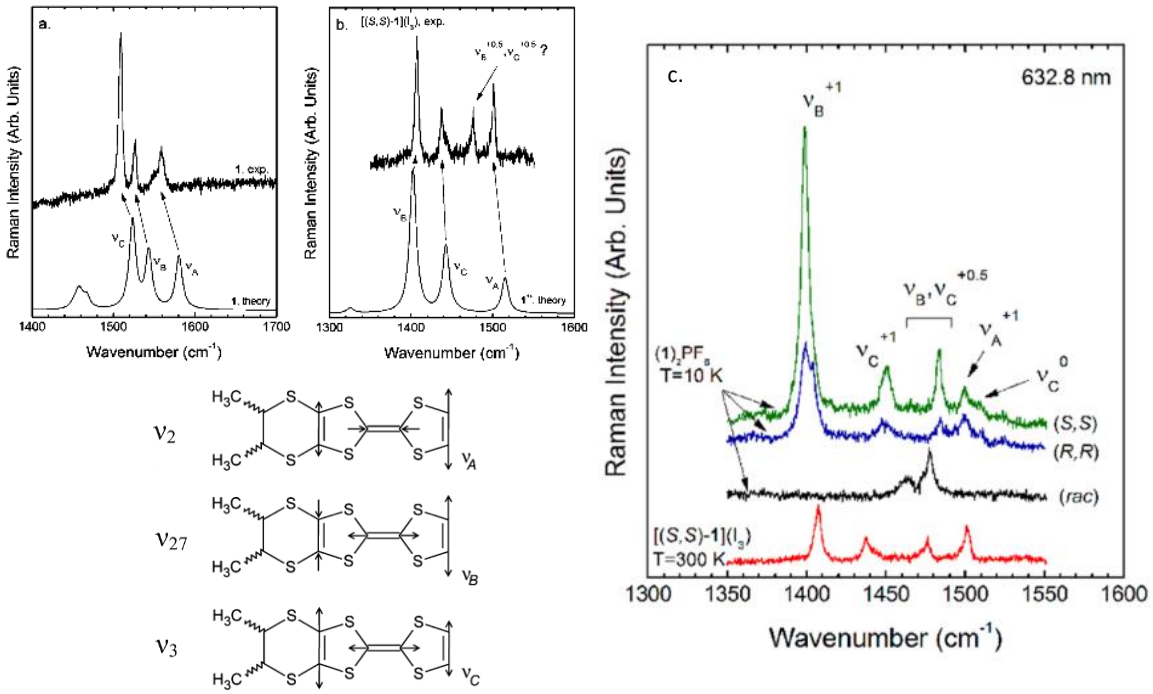

Figure 31: Experimental Raman spectra in the frequency range of the double C=C stretching modes for the neutral DM-EDT-TTF^0 molecule (a) and the iodine ((S,S)-DM-EDT-TTF)I$_3$ salt that features DM-EDT-TTF^{+1} ions (b), together with the respective theoretical spectra of DM-EDT-TTF calculated with the Density Functional Theory (DFT) methods. (c) Raman spectra of ((S,S)-DM-EDT-TTF)$_2$PF$_6$ (S,S), ((R,R)-DM-EDT-TTF)$_2$PF$_6$ (R,R), (rac-DM-EDT-TTF)$_2$PF$_6$ (rac) and ((S,S)-DM-EDT-TTF)I$_3$. The stretching C=C modes' patterns are also shown (with the labels from [81] and [105]) (Reprinted with permission from [81]. Copyright 2013 American Chemical Society).

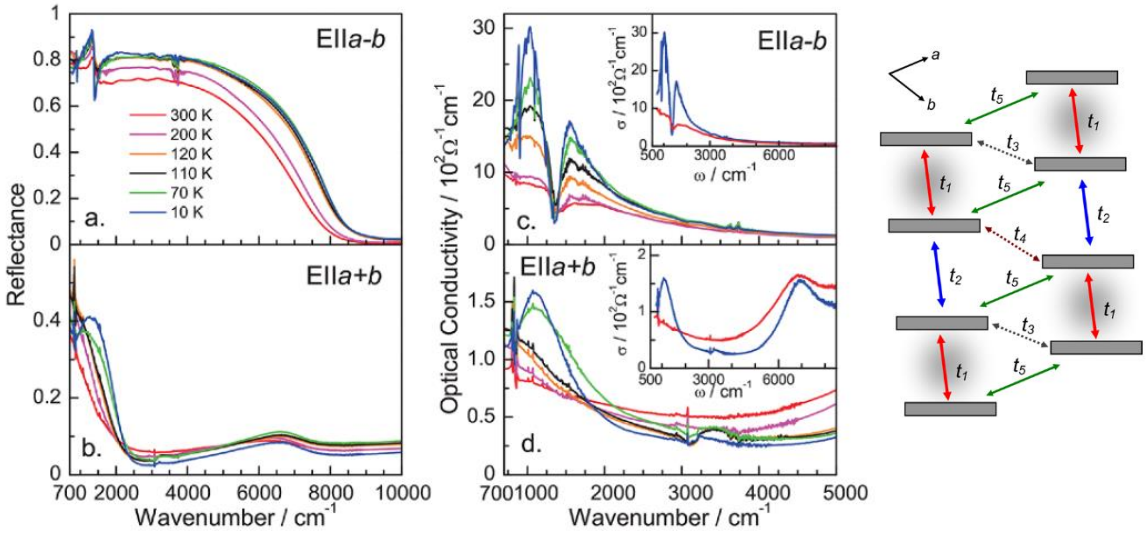

Figure 32: Reflectance (a, b) and optical conductivity spectra (c, d) of the (rac-DM-EDT-TTF)$_2$PF$_6$ salt as a function of temperature. On the right, the arrangement and interactions of molecules in the conducting layer are shown; dimers are marked with grey color, t_1 and t_2 are the transfer integrals within stack, t_5 – the largest transfer integral between stacks, $t_2/t_1 \approx 0.8$, $t_5/t_1 \approx 0.1$ (Reprinted with permission from [105]. Copyright 2017 American Chemical Society).

As the ν_3 mode becomes remarkably enhanced with lowering the temperature, the shape of the optical conductivity spectra in this frequency range has been analyzed using the Fano model (Fig. 33b) [105]. The strong temperature dependence of the ν_3 feature reflects the localized nature of charge carriers in the insulating state. On the other hand, a clear shift towards lower frequencies of the band components of the P-F bonds stretching vibration in the PF_6 anion as observed below 110 K, indicates a notable change in the anionic sublattice (Fig. 33c,d). Such a change most probably affects the hydrogen bonding-type interactions between the anion layer and the conducting layer [81].

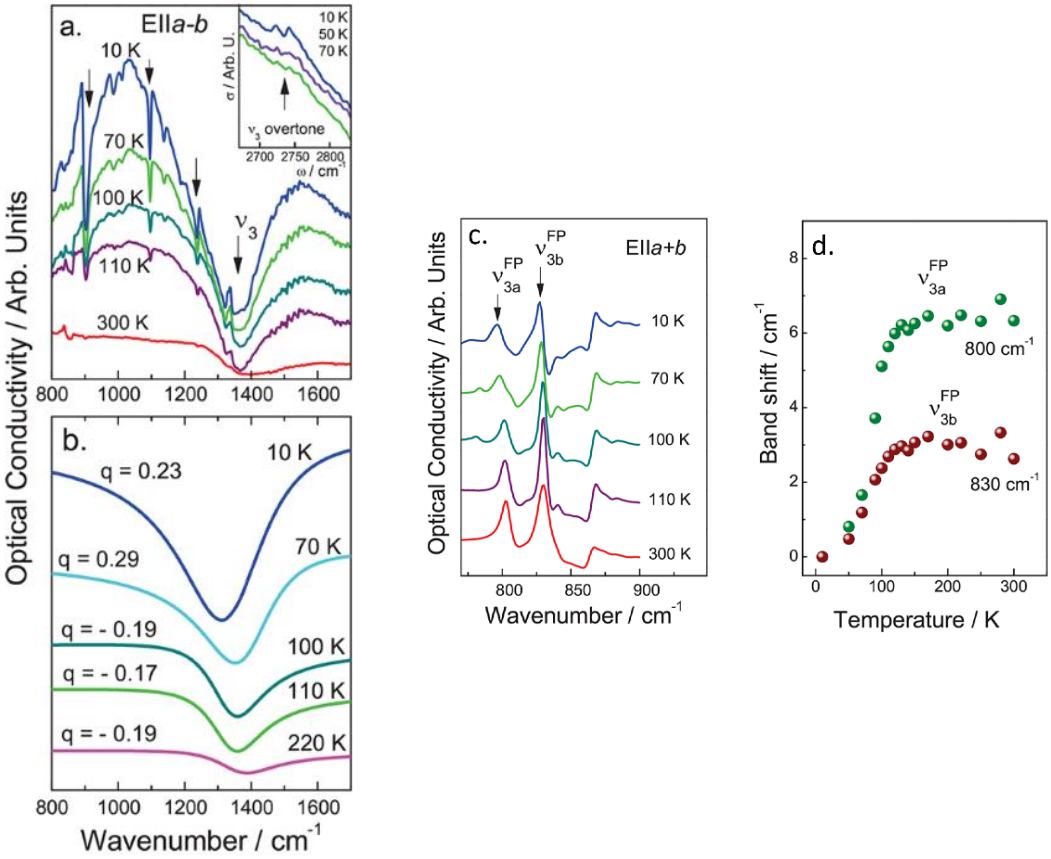

Figure 33: (a) Optical conductivity spectra of (rac-DM-EDT-TTF)$_2$PF$_6$ as a function of temperature in the frequency range of the ν_3 mode; (b) respective spectra calculated using the Fano model. (c) optical conductivity spectra in the range of stretching vibrations of the PF_6 anion. (d) softening of the stretching F-P mode components observed below 110 K (Reprinted with permission from [105]. Copyright 2017 American Chemical Society).

Considering the possible charge-ordered states that are characteristic for weakly dimerized materials we focus on Raman spectra (Fig. 34 shows the spectra measured with two laser excitation lines). A wide band at 1475 cm^{-1} is attributed to the ν_3 and ν_{27} modes of DM-EDT-TTF molecule. The second band centered at 1520 cm^{-1}, broad and unsymmetrical ν_2 mode, has been used to calculate the charge distribution in (rac-DM-EDT-TTF)$_2$PF$_6$ (Fig. 34a,b). By analogy with the BEDT-TTF molecule, it was assumed that ν_2 mode is characterized by a linear frequency dependence on charge. The broadened shape of the mode (Fig. 34c) was modeled using Kubo model, which allowed to estimate the amplitude of charge fluctuation $\Delta\rho \approx 0.25e$ at 10 K (Fig. 34d).

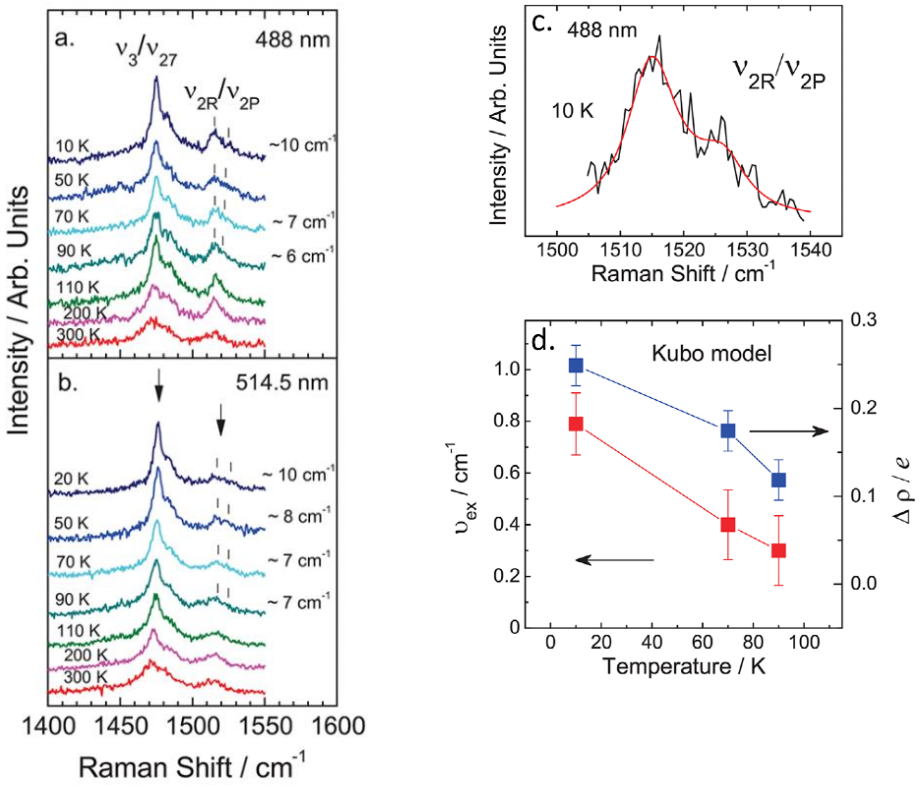

Figure 34: Raman spectra of (rac-DM-EDT-TTF)$_2$PF$_6$ as a function of temperature, measured with the laser lines 488 nm (a) and 514.5 nm (b), together with the results of modeling of the charge-sensitive ν_2 mode components (c) using the Kubo model (d) (Reprinted with permission from [105]. Copyright 2017 American Chemical Society).

The reflectance spectra of (rac-DM-EDT-TTF)$_2$PF$_6$ can be compared with the similar optical properties of the charge-ordered organic conductor β-(meso-DMBEDT-TTF)$_2$PF$_6$ [106], which is superconducting under increased pressure [107]. Following the description of Mori who discusses the CO pattern in such organic conductors from the point of view of the intersite Coulomb V parameters [42], the relationship between charge fluctuations in (rac-DM-EDT-TTF)$_2$PF$_6$ and the estimated values of the Coulomb V interactions in the conducting layer has been suggested [105]. In case of many organic conductors with a layered structure, these interactions are more homogeneous in the conducting layer than the transfer integrals, and their distribution strongly influences the stabilization of a particular charge order [42]. Therefore, we propose that fluctuating charge order within the dimer-Mott insulating phase is stabilized in (rac-DM-EDT-TTF)$_2$PF$_6$ at low temperature due to a specific configuration of intermolecular Coulomb repulsion parameters.

5. Concluding remarks

This review concerned the broadly understood issues of charge localization and superconducting characteristics in low-dimensional organic conductors based on BEDT-TTF donor molecule or unsymmetrical tetrathiafulvalene derivatives. Important contributions have been made with the application of the optical spectroscopy methods that are particularly useful in the field of these materials due to the broad energy range covered by the method, possibility to study both the electronic and

vibrational properties that can be coupled, as well as the microscopic character of the response in the vibrational frequency range. The most important achievements include identification of vibrational bands that are sensitive to superconducting to normal phase transition under magnetic field in the κ-(BEDT-TTF)$_2$X organic conductors. Charge ordering mechanism in β′′-(BEDT-TTF)$_2$$CF_3CH_2SO_3$ and β′′-(BEDT-TTF)$_2$$SF_5CH_2SO_3$, has been explained as related with the dimerization induced with the presence of the hydrogen bonding between the anion and donor layers. Low-temperature charge ordering transition together with the lattice distortion has been confirmed in β′-(BEDT-TTF)$_2$$CF_3CF_2SO_3$ dimer Mott insulator. The effects related with charge fluctuations together with the stabilization of the metal/insulator mixed state have been discovered in the β′′-(BEDT-TTF)$_4$[$(H_3O)Fe(C_2O_4)_3$]·Y organic superconductors. It was shown that (rac-DM-EDT-TTF)$_2$$PF_6$ is a dimer-Mott insulator below the metal-insulator transition at 110 K; detailed analysis of the Raman spectra suggested low-temperature charge fluctuations in this material. With no doubt, experimental observations with the help of the optical spectroscopy methods provide broader understanding of the physical properties of low-dimensional organic conductors.

6. References

[1] F. Sawano, I. Terasaki, H. Mori, T. Mori, M. Watanabe, N. Ikeda, Y. Nogami, and Y. Noda, An organic thyristor, *Nature* 2005, **437**, 522.

[2] W. Little, Possibility of synthesizing an organic superconductor, *Phys. Rev.* 1964, **134**, A1416–A1424.

[3] D. Jérome, A. Mazaud, M. Ribault, and K. Bechgaard, Superconductivity in a synthetic organic conductor (TMTSF)$_2$$PF_6$, *J. Phys. (Paris) Lett.* 1980, **41**, L95.

[4] K. Bechgaard, K. Carneiro, F. B. Rasmussen, M. Olsen, G. Rindorf, C. S. Jacobsen, H. J. Pedersen, and J. C. Scott, Superconductivity in an organic solid. Synthesis, structure, and conductivity of bis (tetramethyltetraselenafulvalenium)perchlorate, (TMTSF)$_2$$ClO_4$, *J. Am. Chem. Soc.* 1981, **103**, 2440-2442.

[5] H. Seo, C. Hotta, and H. Fukuyama, Toward systematic understanding of diversity of electronic properties in low-dimensional molecular solids, *Chem. Rev.* 2004, **104**, 5005.

[6] M. Dressel, and N. Drichko, Optical properties of two-dimensional organic conductors: signatures of charge ordering and correlation effects, *Chem. Rev.* 2004, **104**, 5689.

[7] T. Mori, *Electronic Properties of Organic Conductors*, Springer-Verlag, Japan, 2016.

[8] B. Powell, and R. H. McKenzie, Quantum frustration in organic Mott insulators: from spin liquids to unconventional superconductors, *Phys.: Condens. Matter* 2006, **18**, R827.

[9] A. M. Kini, U. Geiser, H. H. Wang, K. D. Carlson, J. M. Williams, W. K. Kwok, K. G. Vandervoort, J. E. Thompson, D. L. Stupka, D. Jung, and M.-H. Whangbo, A new ambient-pressure organic superconductor, κ-(ET)$_2$Cu[N(CN)$_2$]Br, with the highest transition temperature yet observed (inductive onset T_c = 11.6 K, resistive onset = 12.5 K), *Inorg. Chem.* 1990, **29**, 2555.

[10] M. Lang, F. Steglich, N. Toyota, and T. Sasaki, Fluctuation effects and mixed-state properties of the layered organic superconductors κ-(BEDT-TTF)$_2$Cu(NCS)$_2$ and κ-(BEDT-TTF)$_2$Cu[N(CN)$_2$]Br, *Phys. Rev. B* 1994, **49**, 15227.

[11] T. Yamamoto, H. M. Yamamoto, R. Kato, M. Uruichi, K. Yakushi, H. Akutsu, A. Sato-Akutsu, A. Kawamoto, S. S. Turner, and P. Day, Inhomogeneous site charges at the boundary between the insulating, superconducting, and metallic phases of β′′-type bis-ethylenedithio-tetrathiafulvalene molecular charge-transfer salts, *Phys. Rev. B* 2008, **77**, 205120.

[12] S. Kaiser, M. Dressel, Y. Sun, A. Greco, J. A. Schlueter, G. L. Gard, and N. Drichko, Bandwidth tuning triggers interplay of charge order and superconductivity in two-dimensional organic materials, *Phys. Rev. Lett.* 2010, **105**, 206402.

[13] K. Yakushi, Infrared and Raman studies of charge ordering in organic conductors, BEDT-TTF salts with quarter-filled bands, *Crystals* 2012, **2**, 1291.

[14] J. Merino, and R. H. McKenzie, Superconductivity mediated by charge fluctuations in layered molecular crystals, *Phys. Rev. Lett.* 2001, **87**, 237002.

[15] C. Hotta, Quantum electric dipoles in spin-liquid dimer Mott insulator κ-$ET_2Cu_2(CN)_3$, *Phys. Rev. B* 2010, **82**, 241104.

[16] H. Li, R. T. Clay, and S. Mazumdar, The paired-electron crystal in the two-dimensional frustrated quarter-filled band, *J. Phys.: Condens. Matter* 2010, **22**, 272201.

[17] S. Dayal, R. T. Clay, H. Li, and S. Mazumdar, Paired electron crystal: Order from frustration in the quarter-filled band, *Phys. Rev. B* 2011, **83**, 245106.

[18] T. Koretsune, and C. Hotta, Evaluating model parameters of the κ- and β′-type Mott insulating organic solids, *Phys. Rev. B* 2014, **89**, 045102.

[19] K. Itoh, H. Itoh, M. Naka, S. Saito, I. Hosako, N. Yoneyama, S. Ishihara, T. Sasaki, and S. Iwai, Collective excitation of an electric dipole on a molecular dimer in an organic dimer-Mott insulator, *Phys. Rev. Lett.* 2013, **110**, 106401.

[20] S. Tomić, and M. Dressel, Ferroelectricity in molecular solids: a review of electrodynamic properties, *Rep. Prog. Phys.* 2015, **78**, 096501.

[21] K. Yamamoto, S. Iwai, S. Boyko, A. Kashiwazaki, F. Hiramatsu, C. Okabe, N. Nishi, and K. Yakushi, Strong optical nonlinearity and its ultrafast response associated with electron ferroelectricity in an organic conductor, *J. Phys. Soc. Jpn.* 2008, **77**, 074709.

[22] S. Iguchi, S. Sasaki, N. Yoneyama, H. Taniguchi, T. Nishizaki, and T. Sasaki, Relaxor ferroelectricity induced by electron correlations in a molecular dimer Mott insulator, *Phys. Rev. B* 2013, **87**, 075107.

[23] A. Pustogow, M. Bories, A. Löhle, R. Rösslhuber, E. Zhukova, B. Gorshunov, S. Tomić, J. A. Schlueter, R. Hübner, T. Hiramatsu, Y. Yoshida, G. Saito, R. Kato, T.-H. Lee, V. Dobrosavljević, S. Fratini, and M. Dressel, Quantum spin liquids unveil the genuine Mott state, *Nat. Mater.* 2018, **17**, 773.

[24] M. Dressel, and A. Pustogow, Electrodynamics of quantum spin liquids, *J. Phys.: Condens. Matter* 2018, **30**, 203001.

[25] N. Hassan, S. Cunningham, M. Mourigal, E. I. Zhilyaeva, S. A. Torunova, R. N. Lyubovskaya, J. A. Schlueter, and N. Drichko, Evidence for a quantum dipole liquid state in an organic quasi-two-dimensional material, *Science* 2018, **360**, 1101.

[26] T. Sasaki, Mott-Anderson transition in molecular conductors: Influence of randomness on strongly correlated electrons in the κ-$(BEDT\text{-}TTF)_2X$ system, *Crystals* 2012, **2**, 374.

[27] M. Pinterić, D. R. Góngora, Ž. Rapljenović, T. Ivek, M. Čulo, B. Korin-Hamzić, O. Milat, B. Gumhalter, P. Lazić, M. S. Alonso, W. Li, A. Pustogow, G. G. Lesseux, M. Dressel, and S. Tomić, Electrodynamics in organic dimer insulators close to Mott critical point, *Crystals* 2018, **8**, 190.

[28] E. Coronado, J. R. Galán-Mascarós, C. J. Gómez-Garcia, and V. Laukhin, Coexistence of ferromagnetism and metallic conductivity in a molecule-based layered compound, *Nature* 2000, **408**, 447.

[29] E. Coronado, and P. Day, Magnetic molecular conductors, *Chem. Rev.* 2004, **104**, 5419.

[30] E. Coronado, and J. R. Galán-Mascarós, Hybrid molecular conductors, *J. Mater. Chem.* 2005, **15**, 66.

[31] N. Avarvari, and J. D. Wallis, Strategies towards chiral molecular conductors, *J. Mater. Chem.* 2009, **19**, 4061−4076.

[32] J. Hubbard, Electron correlations in narrow energy bands, *P Roy. Soc. A-Math Phy.* 1963, **276,** 238–257.

[33] M. Imada, A. Fujimori, and Y. Tokura, Metal-insulator transitions, *Rev. Mod. Phys.* 1998, **70**, 1039–1263.

[34] H. Seo and H. Fukuyama, Antiferromagnetic Phases of One-Dimensional Quarter-Filled Organic Conductors, *J. Phys. Soc. Jpn* 1997, **66**, 1249–1252.

[35] T. Mori, Estimation of off-site Coulomb integrals and phase diagrams of charge ordered states in the θ-phase organic conductors *Bull. Chem. Soc. Jpn* 2000, **73**, 2243–2253.

[36] A. C. Jacko, H. Feldner, E. Rose, F. Lissner, M. Dressel, R. Valenti, and H. O. Jeschke, Electronic properties of Fabre charge-transfer salts under various temperature and pressure conditions, *Phys. Rev. B* 2013, **87**, 155139.

[37] M. J. Rozenberg, G. Kotliar, H. Kajueter, G. A. Thomas, D. H. Rapkine, J. M. Honig, and P. Metcalf, Optical conductivity in Mott-Hubbard systems, *Phys. Rev. Lett.* 1995, **75**, 105.

[38] D. Faltermeier, J. Barz, M. Dumm, M. Dressel, N. Drichko, B. Petrov, V. Semkin, R. Vlasova, C. Mézière, and P. Batail, Bandwidth-controlled Mott transition in κ−(BEDT−TTF)$_2$Cu[N(CN)$_2$]Br$_x$Cl$_{1-x}$: Optical studies of localized charge excitations, *Phys. Rev. B* 2007, **76**, 165113.

[39] J. Ferber, K. H. O. Jeschke, and R. Valenti, Unveiling the microscopic nature of correlated organic conductors: The case of κ-(ET)$_2$Cu[N(CN)$_2$]Br$_x$Cl$_{1-x}$, *Phys. Rev. B* 2014, **89**, 205106.

[40] K. Hashimoto, R. Kobayashi, H. Okamura, H. Taniguchi, Y. Ikemoto, T. Moriwaki, S. Iguchi, M. Naka, S. Ishihara, and T. Sasaki, Emergence of charge degrees of freedom under high pressure in the organic dimer-Mott insulator β′−(BEDT−TTF)$_2$ICl$_2$, *Phys. Rev. B* 2015, **92**, 085149.

[41] H. Tajima, S. Kyoden, H. Mori, and S. Tanaka, Estimation of charge-ordering patterns in θ−ET$_2$MM′(SCN)$_4$ (MM′=RbCo,RbZn,CsZn) by reflection spectroscopy, *Phys. Rev. B* 2000, **62**, 9378.

[42] T. Mori, Non-stripe charge order in dimerized organic conductors, *Phys. Rev. B* 2016, **93**, 245104.

[43] M. Dressel, N. Drichko, J. A. Schlueter, and J. Merino, Proximity of the layered organic conductors α−(BEDT−TTF)$_2$MHg(SCN)$_4$ (M=K,NH$_4$) to a charge-ordering transition, *Phys. Rev. Lett.* 2003, **90**, 167002.

[44] S. Kaiser, M. Dressel, Y. Sun, A. Greco, J. A. Schlueter, G. L. Gard, and N. Drichko, Bandwidth tuning triggers interplay of charge order and superconductivity in two-dimensional organic materials, *Phys. Rev. Lett.* 2010, **105**, 206402.

[45] A. Girlando, M. Masino, A. Brillante, R. G. Della Valle, and E. Venuti, BEDT-TTF organic superconductors: The role of phonons, *Phys. Rev. B* 2002, **66**, 100507.

[46] M. J. Rice, Towards the experimental determination of the fundamental microscopic parameters of organic ion-radical compounds, *Solid State Commun.* 1979, **31**, 93–98.

[47] V. M. Yartsev, and A. Graja, Electron–intramolecular vibration coupling in charge-transfer salts studied by infrared spectroscopy, *Int. J. Mod. Phys.* 1998, **12**, 1643–1672.

[48] P. Guionneau, C. Kepert, G. Bravic, D. Chasseau, M. Truter, M. Kurmoo, and P. Day, Determining the charge distribution in BEDT-TTF salts, *Synth. Met.* 1997, **86**, 1973.

[49] A. A. Bardin, unpublished results, 2015.

[50] A. Girlando, M. Masino, J. A. Schlueter, N. Drichko, S. Kaiser, and M. Dressel, Charge-order fluctuations and superconductivity in two-dimensional organic metals, *Phys. Rev. B* 2014, **89**, 174503.

[51] R. Kubo, *Advances in Chemical Physic: Correlation Effects in Atoms and Molecules*, Vol. 14, John Wiley and Sons, Inc.: Hoboken, NJ, USA, 1969.

[52] M. E. Kozlov, K. I. Pokhodnia, and A. A. Yurchenko, Electron molecular vibration coupling in vibrational spectra of BEDT-TTF based radical cation salts, *Spectrochim. Acta Part A* 1989, **45**, 437–444.

[53] J. E. Eldridge, C. C. Homes, J. M. Williams, A. M. Kini, and H. H. Wang, The assignment of the normal modes of the BEDT-TTF electron-donor molecule using the infrared and Raman spectra of several isotopic analogs, *Spectrochim. Acta Part A* 1995, **51**, 947–960.

[54] T. Yamamoto, M. Uruichi, K. Yamamoto, K. Yakushi, A. Kawamoto, and H. Taniguchi, Examination of the charge-sensitive vibrational modes in bis(ethylenedithio)tetrathiafulvalene, *J. Phys. Chem. B* 2005, **109**, 15226–15235.

[55] R. Świetlik, N. D. Kushch, L. A. Kushch, and E. B. Yagubskii, Spectral studies of isostructural organic metals $(BEDT\text{-}TTF)_3(HSO_4)_2$ and $[Ni(dddt)_2]_3(HSO_4)_2$, *Phys. Status Solidi B* 1994, **181**, 499–507.

[56] R. Świetlik, and C. Garrigou-Lagrange, Charge transfer coupling to B_{1u} modes in BEDT-TTF salts, *Synth. Met.* 1993, **55–57**, 2217–2221.

[57] H. Urayama, H. Yamochi, G. Saito, K. Nozawa, T. Sugano, M. Kinoshita, S. Sato, K. Oshima, A. Kawamoto, and J. Tanaka, A new ambient pressure organic superconductor based on BEDT-TTF with T_C higher than 10 K (T_C=10.4 K), *Chem. Lett.* 1988, **17**, 55.

[58] J. M. Williams, A. M. Kini, H. H. Wang, K. D. Carlson, U. Geiser, L. K. Montgomery, G. J. Pyrka, D. M. Watkins, J. M. Kommers, S. J. Boryshuk, A. V. S. Crouch, W. K. Kwok, J. E. Schirber, D. L. Overmyer, D. Jung, and M.-H. Whangbo, From semiconductor-semiconductor transition (42 K) to the highest- T_c organic Superconductor, $\kappa\text{-}(ET)_2Cu[N(CN)_2]CI$ (T_c = 12.5 K), *Inorg. Chem.* 1990, **29**, 3272.

[59] T. Mori, Structural genealogy of BEDT-TTF-based organic conductors I. Parallel molecules: β and β″ phases, *Bull. Chem. Soc. Jpn.* 1998, **71**, 2509–2526.

[60] T. Yamamoto, M. Uruichi, K. Yakushi, and A. Kawamoto, Charge ordering state of $\beta''\text{-}(ET)_3(HSO_4)_2$ and $\beta''\text{-}(ET)_3(ClO_4)_2$ by temperature-dependent infrared and Raman spectroscopy, *Phys. Rev. B* 2006, 73, 125116.

[61] B. H. Ward, J. A. Schlueter, U. Geiser, H. H. Wang, E. Morales, J. P. Parakka, S. Y. Thomas, J. M. Williams, P. G. Nixon, R. W. Winter, G. L. Gard, H.-J. Koo, and M.-H. Whangbo, Comparison of the crystal and electronic structures of three 2:1 salts of the organic donor molecule BEDT-TTF with pentafluorothiomethylsulfonate anions $SF_5CH_2SO_3^-$, $SF_5CHFSO_3^-$, and $SF_5CF_2SO_3^-$, *Chem. Mater.* 2000, **12**, 343.

[62] J. A. Schlueter, B. H. Ward, U. Geiser, H. H. Wang, A. M. Kini, J. P. Parakka, E. Morales, H.-J. Koo, M.-H. Whangbo, R. W. Winter, J. Mohtasham and G. L. Gard, Crystal structure, physical properties and electronic structure of a new organic conductor $\beta''\text{-}(BEDT\text{-}TTF)_2SF_5CHFCF_2SO_3$, *J. Mater. Chem.* 2001, **11**, 2008.

[63] U. Geiser, J. A. Schlueter, H. H. Wang, A. M. Kini, J. M. Williams, P. P. Sche, H. I. Zakowicz, M. L. Vanzile, J. D. Dudek, P. G. Nixon, R. W. Winter, G. L. Gard, J. Ren, and M.-H. Whangbo, Superconductivity at 5.2 K in an electron donor radical salt of bis(ethylenedithio)tetrathiafulvalene (BEDT-TTF) with the novel polyfluorinated organic anion $SF_5CH_2CF_2SO_3^-$, *J. Am. Chem. Soc.* 1996, **118**, 9996.

[64] I. Olejniczak, R. Wesołowski, H. O. Jeschke, R. Valentí, B. Barszcz, and J. A. Schlueter, Charge ordering and low-temperature lattice distortion in the $\beta'\text{-}(BEDT\text{-}TTF)_2CF_3CF_2SO_3$ dimer Mott insulator, *Phys. Rev. B* 2020, **101**, 035150.

[65] I. Olejniczak, B. Barszcz, A. Szutarska, A. Graja, R. Wojciechowski, J.A. Schlueter, A.N. Hata, and B.H. Ward, Infrared and Raman spectra of $\beta''\text{-}(BEDT\text{-}TTF)_2RCH_2SO_3$ (R = SF_5, CF_3): dimerization related to hydrogen bonding, *Phys. Chem. Chem. Phys.* 2009, **11**, 3910-3920.

[66] M. Kurmoo, A. W. Graham, P. Day, S. J. Coles, M. B. Hursthouse, J. L. Caulfield, J. Singleton, F. L. Pratt, W. Hayes, L. Ducasse, and P. Guionneau, Superconducting and semiconducting magnetic charge transfer salts: $(BEDT\text{-}TTF)_4AFe(C_2O_4)_3{\cdot}C_6H_5CN$ (A = H_2O, K, NH_4), *J. Am. Chem. Soc.* 1995, **117**, 12209.

[67] S. S. Turner, P. Day, K. M. A. Malik, M. B. Hursthouse, S. J. Teat, E. J. MacLean, L. Martin, and S. A. French, Effect of included solvent molecules on the physical properties of the paramagnetic charge transfer salts β′′-(bedt-ttf)$_4$[(H$_3$O)Fe(C$_2$O$_4$)$_3$]·Solvent (bedt-ttf = Bis(ethylenedithio)tetrathiafulvalene), *Inorg. Chem.* 1999, **38**, 3543.

[68] H. Akutsu, A. Akutsu-Sato, S. S. Turner, D. Le Pevelen, P. Day, V. Laukhin, A.-K. Klehe, J. Singleton, D. A. Tocher, M. R. Probert, and J. A. K. Howard, Effect of included guest molecules on the normal state conductivity and superconductivity of β′′-(ET)$_4$[(H$_3$O)Ga(C$_2$O$_4$)$_3$]·G (G = Pyridine, Nitrobenzene), *J. Am. Chem. Soc.* 2002, **124**, 12430.

[69] E. Coronado, S. Curreli, C. Giménez-Saiz, and J. Gómez-Garcia, A novel paramagnetic molecular superconductor formed by bis(ethylenedithio)tetrathiafulvalene, tris(oxalato)ferrate(iii) anions and bromobenzene as guest molecule: ET$_4$[(H$_3$O)Fe(C$_2$O$_4$)$_3$]·C$_6$H$_5$Br, *J. Mater. Chem.* 2005, **15**, 1429.

[70] T. G. Prokhorova, L. I. Buravov, E. B. Yagubskii, L. V. Zorina, S. S. Khasanov, S. V. Simonov, R. P. Shibaeva, A. V. Korobenko, and V. N. Zverev, Effect of electrocrystallization medium on quality, structural features, and conducting properties of single crystals of the (BEDT-TTF)$_4$AI[FeIII(C$_2$O$_4$)$_3$]·G family, *CrystEngComm* 2011, **13**, 537.

[71] T. G. Prokhorova, S. S. Khasanov, L. V. Zorina, L. I. Buravov, V. A. Tkacheva, A. A. Baskakov, R. B. Morgunov, M. Gener, E. Canadell, R. P. Shibaeva, and E. B. Yagubskii, Molecular Metals Based on BEDT-TTF Radical Cation Salts with Magnetic Metal Oxalates as Counterions: β″-(BEDT-TTF)$_4$A[M(C$_2$O$_4$)$_3$]·DMF (A = NH_4^+, K+; M = Cr^{III}, Fe^{III}), *Adv. Funct. Mater.* 2003, **13**, 403.

[72] A. Akutsu-Sato, H. Akutsu, J. Yamada, S. Nakatsuji, S. S. Turner, and P. Day, Suppression of superconductivity in a molecular charge transfer salt by changing guest molecule: β″-(BEDT-TTF)$_4$[(H$_3$O) Fe(C$_2$O$_4$)$_3$](C$_6$H$_5$CN)$_x$(C$_5$H$_5$N)$_{1-x}$, *J. Mater. Chem.* 2007, **17**, 2497.

[73] L. V. Zorina, T. G. Prokhorova, S. V. Simonov, S. S. Khasanov, R. P. Shibaeva, A. I. Manakov, V. N. Zverev, L. I. Buravov, and E. B. Yagubskii, Structure and magnetotransport properties of the new quasi-two-dimensional molecular metal β″-(BEDT-TTF)$_4$H$_3$O[Fe(C$_2$O$_4$)$_3$] · C$_6$H$_4$Cl$_2$, *J. Exp. Theor. Phys.* 2008, **106**, 347.

[74] L. V. Zorina, S. S. Khasanov, S. V. Simonov, R. P. Shibaeva, P. O. Bulanchuk, V. N. Zverev, E. Canadell, T. G. Prokhorova, and E. B. Yagubskii, Structural phase transition in the β″-(BEDT-TTF)$_4$H$_3$O[Fe(C$_2$O$_4$)$_3$]·G crystals (where G is a guest solvent molecule), *CrystEngComm* 2012, **14**, 460.

[75] F. Pop, P. Auban-Senzier, E. Canadell, G. L. J. A. Rikken, and N. Avarvari, Electrical magnetochiral anisotropy in a bulk chiral molecular conductor, *Nat. Commun.* 2014, **5**, 3757.

[76] A. Terzis, A. Hountas, B. Hilti, G. Mayer, J. S. Zambounis, D. J. Lagouvardos, V. Kakoussis, G. Mousdid, and G. C. Papavassiliou, Crystal structures and properties of some cation radicals EDOMDTTTF, EDOVDTTTF, EDOBTTF, EDOPDSDTF, EDODMPTTF, BEDTTTF and BMDTTTF, *Synth. Met.* 1991, **41–43**, 1715.

[77] G. C. Papavassiliou, D. J. Lagouvardos, A. Terzis, C. P. Raptopoulou, B. Hilti, W. Hofherr, J. S. Zambounis, G. Rihs, J. Pfeiffer, P. Delhaès, K. Murata, N. A. Fortune, and N. Shirakawa, Conducting and superconducting salts based on BEDTTTF and on some unsymmetrical tetrachalcogenafulvalenes, *Synth. Met.* 1995, **70**, 787.

[78] I. Olejniczak, J.L. Musfeldt, G.C. Papavassiliou and G.A. Mousdis, Optical investigation of a τ-phase organic molecular conductor: τ-(EDO-(S,S)-DMEDT-TTF)$_2$(AuBr$_2$)(AuBr$_2$)$_y$ with y≈0.75, *Phys. Rev. B* 2000, **62**, 15634-15639.

[79] G. C. Papavassiliou, D. J. Lagouvardos, J. S. Zambounis, A. Terzis, C. P. Raptopoulou, K. Murata, N. Shirakawa, L. Ducasse, and P. Delhaès, Structural and physical properties of τ-(EDO-S,S-DMEDT-TTF)$_2$(AuBr$_2$)$_1$(AuBr$_2$)$_y$, *Mol. Cryst. Liq. Cryst.* 1996, **285**, 83.

[80] G. C. Papavassiliou, D. J. Lagouvardos, I. Koutselas, K. Murata, A. Graja, I. Olejniczak, J. S. Zambounis, L. Ducasse, and J. P. Ulmet, Structural and physical properties of τ-(P-S, S- DMEDT-TTF)$_2$(AuBr$_2$)$_1$(AuBr$_2$)$_{0.75}$ and τ-(EDO-S, S-DMEDT-TTF)$_2$(AuBr$_2$)$_1$(AuBr$_2$)$_{0.75}$, 2D conductors, *Synth. Met.* 1997, **86**, 2043.

[81] F. Pop, P. Auban-Senzier, A. Frąckowiak, K. Ptaszyński, I. Olejniczak, J.D. Wallis, E. Canadell, and N. Avarvari, Chirality driven metallic versus semiconducting behavior in a complete series of radical cation salts based on dimethyl-ethylenedithio-tetrathiafulvalene (DM-EDT-TTF), *J. Am. Chem. Soc.* 2013, **135**, 17176-17186.

[82] K. Yamaji, *Solid State Commun.* 1987, On the mechanism of superconductivity in the organic conductors composed of TTF-analogs, **61**, 413.

[83] H. Elsinger, J. Wosnitza, S. Wanka, J. Hagel, D. Schweitzer, and W. Strunz, κ−(BEDT−TTF)$_2$Cu[N(CN)$_2$]Br: A fully gapped strong-coupling superconductor, *Phys. Rev. Lett.* 2000, **84**, 6098.

[84] J. Müller, M. Lang, R. Helfrich, F. Steglich, and T. Sasaki, High-resolution ac-calorimetry studies of the quasi-two-dimensional organic superconductor κ−(BEDT−TTF)$_2$Cu(NCS)$_2$, *Phys. Rev. B* 2002, **65**, 140509.

[85] T. S. Nunner, J. Schmalian, and K. H. Bennemann, Influence of electron-phonon interaction on spin-fluctuation-induced superconductivity, *Phys. Rev. B* 1999, **59**, 8859.

[86] A. Lanzara, P. V. Bogdanov, X. J. Zhou, S. A. Kellar, D. L. Feng, E. D. Lu, T. Yoshida, H. Elsaki, A. Fujimori, K. Kishio, J.-I. Shimoyama, T. Noda, S. Uchida, Z. Hussain, and Z.-X. Shen, Evidence for ubiquitous strong electron–phonon coupling in high-temperature superconductors, *Nature* 2001, **412**, 510.

[87] O. Gunnarsson, Superconductivity in fullerides, *Rev. Mod. Phys.* 1997, **69**, 575.

[88] I. Olejniczak, J. Choi, J.L. Musfeldt, Y.J. Wang, J.A. Schlueter, and R.A. Klemm, Magnetic field dependent vibrational modes in κ-(ET)$_2$Cu(SCN)$_2$, *Phys. Rev. B* 2003, **67**, 174502/1-6.

[89] A. M. Kini, K. D. Carlson, H. H. Wang, J. A. Schlueter, J. D. Dudek, S. A. Sirchio, U. Geiser, K. R. Lykke, and J. M. Williams, Determination of a mass isotope effect on Tc in an electron-donor-based organic superconductor, κ-(ET)$_2$Cu(NCS)$_2$, where ET represents bis(ethylenedithio)tetrathiafulvalene, *Physica C* 1996, **264**, 81.

[90] J. Choi, J.L. Musfeldt, I. Olejniczak, Y.J. Wang, J.A. Schlueter, and A.M. Kini, Magnetic field dependent vibrational modes in isotopically decorated κ-(ET)$_2$Cu(SCN)$_2$, *Phys. Rev. B* 2003, **68**, 214523/1-6.

[91] M. Lang, F. Steglich, N. Toyota, and T. Sasaki, Fluctuation effects and mixed-state properties of the layered organic superconductors κ-(BEDT-TTF)$_2$Cu(NCS)$_2$ and κ-(BEDT-TTF)$_2$Cu[N(CN)$_2$]Br, *Phys. Rev. B* 1994, **49**, 15227.

[92] U. Welp, S. Fleshler, W. K. Kwok, G. W. Crabtree, K. D. Carlson, H. H. Wang, U. Geiser, J. M. Williams, and V. M. Hitsman, Weak ferromagnetism in κ-(ET)$_2$Cu[N(CN)$_2$]Cl, where (ET) is bis(ethylenedithio)tetrathiafulvalene *Phys. Rev. Lett.* 1992 **69**, 840.

[93] R. Wesołowski, J. T. Haraldsen, J. Cao, J. L. Musfeldt, I. Olejniczak, J. Choi, Y. J. Wang, and J. A. Schlueter, Understanding the totally symmetric intramolecular vibrations in κ-phase organic superconductors, *Phys. Rev. B* 2005, **71**, 214514/1-5.

[94] J. L. Musfeldt, R. Świetlik, I. Olejniczak, J. E. Eldridge, and U. Geiser, Understanding electron-molecular vibrational coupling in organic molecular solids: Experimental evidence for strong coupling of the 890−cm−1 mode in ET-based materials, *Phys. Rev. B* 2005, **72**, 014516.

[95] M. Meneghetti, C. Pecile, K. Yakushi, K. Yamamoto, K. Kanoda, and K. Hiraki, Study of the phase transitions of (DI-DCNQI)$_2$M (M=Ag, Li,Cu) through the analysis of the temperature-dependent vibronic and vibrational infrared absorptions, *J. Solid State Chem.* 2002, **168**, 632–638.

[96] T. Yamamoto, H. M. Yamamoto, R. Kato, M. Uruichi, K. Yakushi, H. Akutsu, A. Sato-Akutsu, A. Kawamoto, S. S. Turner, and P. Day, Inhomogeneous site charges at the boundary between the insulating, superconducting, and metallic phases of β′′-type bis-ethylenedithio-tetrathiafulvalene molecular charge-transfer salts, *Phys. Rev. B* 2008, **77**, 205120.

[97] A. Pustogow, K. Treptow, A. Rohwer, Y. Saito, M. Sanz Alonso, A. Löhle, J. A. Schlueter, and M. Dressel, Charge order in β′′-phase BEDT-TTF salts, *Phys. Rev. B* 2019, **99**, 155144.

[98] A. F. Bangura, A. I. Coldea, J. Singleton, A. Ardavan, A. Akutsu-Sato, H. Akutsu, S. S. Turner, P. Day, Y. Yamamoto, and K. Yakushi, Robust superconducting state in the low-quasiparticle-density organic metals β′′−(BEDT−TTF)$_4$[(H$_3$O)M(C$_2$O$_4$)$_3$]·Y: Superconductivity due to proximity to a charge-ordered state, *Phys. Rev. B* 2005, **72**, 014543.

[99] A. Gambardella, M. Salluzzo, R. Di Capua, M. Affronte, C. Giménez-Saiz, C. J. Gómez-Garcia, E. Coronado, and R. Vaglio, Scanning tunnelling spectroscopy study of paramagnetic superconducting β"-ET$_4$[(H$_3$O)Fe(C$_2$O$_4$)$_3$]·C$_6$H$_5$Br crystals, *J. Phys. Condens. Matter* 2010, **22**, 175701.

[100] L. V. Zorina, S. S. Khasanov, S. V. Simonov, R. P. Shibaeva, V. N. Zverev, E. Canadell, T. G. Prokhorova, and E. B. Yagubskii, Coexistence of two donor packing motifs in the stable molecular metal α-'pseudo-κ'-(BEDT-TTF)$_4$(H$_3$O)[Fe(C$_2$O$_4$)$_3$]·C$_6$H$_4$Br$_2$, *CrystEngComm* 2011, **13**, 2430.

[101] I. Olejniczak, A. Frąckowiak, R. Świetlik, T. G. Prokhorova, and E. B. Yagubskii, Charge fluctuations and ethylene groups ordering transition in the β"-(BEDT-TTF)$_4$[(H$_3$O)Fe(C$_2$O$_4$)$_3$]·Y molecular charge-transfer salts, *ChemPhysChem* 2013, **14**, 3925-3935.

[102] J.-P. Pouget, P. Alemany, and E. Canadell, Donor-anion interactions in quarter-filled low-dimensional organic conductors, *Mater. Horiz.* 2018, **5**, 590.

[103] M. Sawada, S. Fukuoka, and A. Kawamoto, Coupling of molecular motion and electronic state in the organic molecular dimer Mott insulator β′-(BEDT-TTF)$_2$ICl$_2$, *Phys. Rev. B* 2018, **97**, 045136.

[104] J. Merino, M. Dumm, N. Drichko, M. Dressel, and Ross H. McKenzie, Quasiparticles at the verge of localization near the Mott metal-insulator transition in a two-dimensional material, *Phys. Rev. Lett.* 2008, **100,** 086404.

[105] I. Olejniczak, A. Frąckowiak, K. Ptaszyński, F. Pop, and N. Avarvari, Charge fluctuations in the dimer-Mott insulating state of (rac-DM-EDT-TTF)$_2$PF$_6$, *J. Phys. Chem. C* 2017, **121**, 21975-21984

[106] R. Okazaki, Y. Ikemoto, T. Moriwaki, T. Shikama, K. Takahashi, H. Mori, H. Nakaya, T. Sasaki, Y. Yasui, and I. Terasaki, Optical conductivity measurement of a dimer Mott-insulator to charge-order phase transition in at two-dimensional quarter-filled organic salt compound, *Phys. Rev. Lett.* 2013, **111**, 217801.

[107] S. Kimura T. Maejima, H. Suzuki, R. Chiba, H. Mori, T. Kawamoto, T. Mori, H. Moriyama, Y. Nishioe, and K. Kajita, A new organic superconductor β-(meso-DMBEDT-TTF)$_2$PF$_6$, *Chem. Commun.* 2004, 2454.